

Squeezing of a nanomechanical resonator by quantum nondemolition measurement and feedback

Rusko Ruskov,^{1,*} Keith Schwab,² and Alexander N. Korotkov¹

¹*Department of Electrical Engineering, University of California, Riverside, California 92521, USA*

²*Laboratory for Physical Sciences, 8050 Greenmead Drive, College Park, Maryland 20740, USA*

(Received 22 November 2004; revised manuscript received 31 January 2005; published 9 June 2005)

We analyze squeezing of the nanoresonator state produced by periodic measurement of position by a quantum point contact or a single-electron transistor. The mechanism of squeezing is the stroboscopic quantum nondemolition measurement generalized to the case of continuous measurement by a weakly coupled detector. The magnitude of squeezing is calculated for the harmonic and stroboscopic modulations of measurement, taking into account detector efficiency and nanoresonator quality factor. We also analyze the operation of the quantum feedback, which prevents fluctuations of the wave packet center due to measurement back-action. Verification of the squeezed state can be performed in almost the same way as its preparation; a similar procedure can also be used for the force detection with sensitivity beyond the standard quantum limit.

DOI: 10.1103/PhysRevB.71.235407

PACS number(s): 85.85.+j, 03.65.Ta, 73.23.-b

I. INTRODUCTION

Recent advances in fabrication of high-frequency nanomechanical resonators¹⁻⁵ (see also Refs. 6 and 7) make the direct observation of their quantum behavior possible in the nearest future. Resonator frequency $\omega_0/2\pi$ slightly over 1 GHz has been already demonstrated.³ For such a resonator the condition $T < \hbar\omega_0$ (we use $k_B=1$) is satisfied at temperature T below ~ 50 mK, which is within routine experimental range. Actually, even in the case $T \gg \hbar\omega_0$ the quantum behavior is in principle observable⁸ if $T\tau_m/Q \lesssim \hbar$, where Q is the resonator quality factor and τ_m is the typical measurement time. This condition can be satisfied even for a MHz-range resonator with large Q -factor, if measured with a good sensitivity which translates into small τ_m . There is a rapid experimental progress in monitoring the oscillating position of a nanoresonator using radio-frequency single-electron transistor (RF-SET) (Ref. 4 and 5) or quantum point contact (QPC) (Ref. 9) (at present the RF-SET seems to be much more efficient; both solid-state techniques have some advantages compared to more traditional optical monitoring^{10(a),11}). In particular, the position measurement accuracy Δx within the factor 5.8 from the standard quantum limit (SQL) Δx_0 has been demonstrated⁵ using the RF-SET; here $\Delta x_0 = \sqrt{\hbar/2m\omega_0}$ is the width (standard deviation) of the ground state of the oscillator with mass m . Anticipating future progress in measurement precision, in this paper we discuss a way of performing measurement with accuracy better than Δx_0 .

Such measurement implies squeezing of the nanoresonator state and requires using some tricks to avoid the effect of quantum back-action from the detector which normally leads to the SQL.⁸ Actually, an instantaneous position measurement by a strongly coupled detector can in principle be made with precision Δx better than Δx_0 (orthodox projection, for example, implies $\Delta x=0$); however, the limitation by the SQL arises for consecutive measurements and also for measurement by a weakly coupled detector, which is necessarily continuous. The well-known way to overcome the SQL limitation is to use quantum nondemolition (QND)

measurements.^{8,12-14} The general idea of a QND measurement is to avoid measuring (or obtaining any information on) the magnitude conjugated to the magnitude of interest, and therefore to avoid the corresponding back-action. An important implementation of this idea is the “stroboscopic” measurement of the oscillator position.^{12,13} Suppose the position x_1 is measured (instantaneously) with a finite precision Δx , which necessarily disturbs the momentum according to the Heisenberg uncertainty principle $\Delta p \geq \hbar/2\Delta x$. Normally this momentum change would affect the result of the next position measurement x_2 and would limit the accuracy for the position difference x_2-x_1 , leading to the SQL for this magnitude. However, if the second measurement is performed exactly one oscillation period after the first one, the oscillator returns to its initial state, and therefore the momentum change does not affect the accuracy of the x_2-x_1 measurement. Such stroboscopic measurement gives no information related to the momentum, and this is exactly the reason why the effect of quantum back-action is avoided.^{8,12-14}

The QND measurements have been mainly discussed in relation to detection of very weak classical forces, in particular gravitational waves (see, e.g., Refs. 15–17; see also Ref. 18). Recently the idea of QND measurements has been also applied to solid-state mesoscopic structures (see, e.g., Refs. 19–21). Among other recent developments (total number of papers on QND measurements is about half a thousand) let us mention the experiment on atomic spin-squeezing using the QND measurement and real-time quantum feedback.²² Squeezing of a nanomechanical resonator using the QND measurement by QPC or SET and quantum feedback has been proposed in our recent Proceedings paper;²³ the present paper is a more complete analysis of this proposal.

Measurement of the nanoresonator position by the SET or QPC has already received a significant theoretical attention.^{7,24-32} In particular, it was shown that the process of measurement transfers the energy from the detector to the nanoresonator leading to its “heating.”^{24,25} A possible way to prevent such heating is using the quantum feedback control of the nanoresonator^{30,33} (other ideas for cooling have been proposed in Refs. 34 and 35).

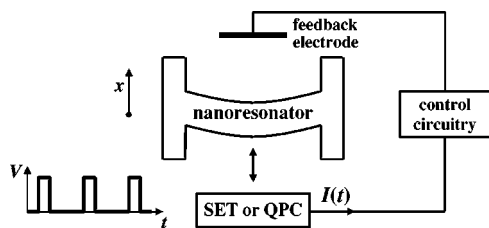


FIG. 1. Simplified schematic of the nanoresonator, which position x is measured by a single electron transistor or a quantum point contact. Stroboscopic modulation of the detector voltage $V(t)$ with frequency $2\omega_0/n$ leads to nanoresonator state squeezing. Detector output $I(t)$ is used to monitor nanoresonator position. The quantum feedback loop keeps the center of the nanoresonator wavepacket close to $x=0$.

The general idea of quantum feedback is very similar to classical feedback and is based on the continuous monitoring of the system state and its continuous control towards a desired state. However, the nontrivial part is accurate monitoring of evolution of the quantum state (wave function in the ideal case), which requires explicit account of the detector back-action. The quantum feedback of mesoscopic solid-state systems is a relatively new subject,³⁶ though in quantum optics the quantum feedback has been proposed more than a decade ago³⁷ and has been already realized experimentally.²² The quantum feedback analyzed in Ref. 30 assumes continuous monitoring of the nanoresonator state with constant “strength” of measurement and allows cooling of the nanoresonator practically down to the ground state. However, it does not allow squeezing of the nanoresonator state (below Δx_0), except in the unrealistic case of a strong coupling between the nanoresonator and detector.

Besides curiosity, the interest to nanoresonator squeezing is justified by its importance for the ultrasensitive force detection. Nanoresonator squeezing by periodic modulation of the spring constant at twice the flexural frequency has been proposed and analyzed in Refs. 38 and 7 (this proposal is to some extent a scaled down version of the proposal³⁹ for gravitational-wave detection and experiment on classical thermomechanical noise squeezing⁴⁰). Nanoresonator squeezing by reservoir engineering (by coupling to a qubit and illumination with two microwaves) has been proposed in Ref. 41. We would like to notice that to be useful for an ultrasensitive force detection, the preparation of a squeezed state should in any case be complemented by the measurement stage after the force has acted on the nanoresonator; the most natural way for this measurement is using the RF-SET (or QPC) as a detector, and such measurement of a squeezed state is not trivial (unless detector is strongly coupled).

In this paper we analyze the nanoresonator squeezing produced by measuring the nanoresonator position (Fig. 1) with the measurement strength modulated in time²³ (for example, modulating the bias voltage of the QPC or RF-SET), so the stages of the squeezed state preparation and its measurement are essentially similar. We show that even for a weak coupling with detector, a significant squeezing of the nanoresonator state can be achieved when the modulation frequency ω is close to $2\omega_0/n$, $n=1,2,\dots$.

The mechanism of this effect is exactly the physics of stroboscopic QND measurements^{12,13} and can be easily un-

derstood for the case of short measurement pulses applied periodically, for example, once per oscillation period ($n=2$). Each measurement pulse gives us some (though quite imprecise) information on the nanoresonator position x and correspondingly reduces the width of the resonator density matrix in x -domain. Between the pulses the resonator undergoes free evolution, which returns the density matrix into exactly the same state one period later (neglecting effects of finite Q -factor and unharmonicity). Therefore, the free evolution produces no effect, and measurement pulses are “stacked one upon another,” so that the measurement strength adds up, and many imprecise measurements become equivalent to one very precise measurement. When the precision of such measurement becomes better than Δx_0 , the x -width (uncertainty) of the resonator state (density matrix) necessarily becomes smaller than the ground state width, so the squeezed state is produced. Exactly the same mechanism of squeezing works when the measurement pulses are separated by integer number of oscillation periods (even n) or by an odd number of half-periods (odd n) since the free evolution during a half-period results only in the sign change for position and momentum.

Notice that even though the measurement squeezes the resonator position x , free evolution between pulses makes it a “breathing” mode, so that x -width oscillates in time (with frequency $2\omega_0$) becoming periodically larger and smaller than Δx_0 ; correspondingly the momentum uncertainty of the resonator also oscillates and becomes squeezed below $\hbar/2\Delta x_0$ periodically. Because of these oscillations, squeezing is usually considered in the rotating frame, so what is usually discussed is squeezing of one of two quadrature amplitudes, which can be translated via free evolution into the position and momentum at time $t=0$. However, in this paper we prefer to consider explicitly the oscillating time dependence of the position and momentum uncertainty, and in this sense we often use terminology of oscillating in time squeezing of position (or momentum).

Finite duration of each measurement pulse prevents complete self-compensation of free evolution and consequently prevents infinite accumulation of the squeezing degree; instead, squeezing saturates after initial transient period. An explicit account of finite pulse duration for continuous measurement by a weakly coupled detector is one of the main differences between our formalism and the standard analysis of stroboscopic QND measurements.^{12,13}

Finite duration of measurement pulses also leads to a random motion (diffusionlike) of the wave packet center at the moments of maximum x -squeezing. This can be explained as a consequence of random momentum kicks during measurement pulses, which are the quantum back-action price for x -measurement. Since the free evolution between the pulses is not cancelled exactly, momentum kicks lead to gradual x -evolution as well. This effect causes gradual “heating” of the nanoresonator. If not stopped by the damping due to finite Q -factor, the resonator energy will grow up to the effective detector temperature which is on the order of the detector voltage^{7,25} and is typically very large compared to $\hbar\omega_0$. This heating can be prevented by using the quantum feedback which can keep the wave packet center near zero; such feedback has been analyzed by Hopkins *et al.*,³⁰ and we will

basically follow their analysis in the present paper.

Finite Q -factor of the nanoresonator, finite temperature of the environment, and resonator unharmonicity obviously decrease the maximum achievable squeezing. In this paper we consider the effects of the Q -factor and temperature (though for many results they are neglected), but we do not consider unharmonicity. We also do not analyze explicitly the use of the squeezed state for the ultrasensitive force detection; however, we discuss the procedure of squeezed state verification, which is a closely related topic. In the next section we develop Bayesian formalism for the analysis of our setup; it is shown to coincide with the formalism of conditional evolution used in previous papers, in particular in Refs. 33 and 30. Measurement modulation and simplified equations for Gaussian states are discussed in Sec. III; Sec. IV is devoted to the calculation of squeezing; quantum feedback is analyzed in Sec. V; verification of the squeezed state is discussed in Sec. VI; and Sec. VII is the conclusion.

II. MODEL AND BAYESIAN FORMALISM

For simplicity we consider the nanoresonator (Fig. 1) measured by the low-transparency QPC (though our results are applicable to the RF-SET as well), and the system Hamiltonian is

$$\mathcal{H} = \mathcal{H}_0 + \mathcal{H}_{\text{det}} + \mathcal{H}_{\text{int}} + \mathcal{H}_{\text{env}} + \mathcal{H}_{\text{fb}}, \quad (1)$$

where the first term describes the oscillator:

$$\mathcal{H}_0 = \frac{\hat{p}^2}{2m} + \frac{m\omega_0^2 \hat{x}^2}{2} \quad (2)$$

(\hat{p} and \hat{x} being the momentum and position operators), the last term

$$\mathcal{H}_{\text{fb}} = -\mathcal{F}\hat{x} \quad (3)$$

describes the feedback control of the nanoresonator by applying the force $\mathcal{F}(t)$. \mathcal{H}_{det} and \mathcal{H}_{int} correspond to the detector and its interaction with the nanoresonator similar to Refs. 42 and 25:

$$\mathcal{H}_{\text{det}} = \sum_l E_l a_l^\dagger a_l + \sum_r E_r a_r^\dagger a_r + \sum_{l,r} (M a_r^\dagger a_l + \text{h.c.}), \quad (4)$$

$$\mathcal{H}_{\text{int}} = \sum_{l,r} (\Delta M \hat{x} a_r^\dagger a_l + \text{h.c.}). \quad (5)$$

Finally, \mathcal{H}_{env} describes nanoresonator interaction with phonon bath at temperature T ; this interaction is assumed to be weak and leads to a large quality factor $Q \gg 1$. In Eqs. (4) and (5) $a_{l,r}^\dagger$ and $a_{l,r}$ are the creation and annihilation operators for two electrodes of the QPC, for simplicity we assume no relative phase between the tunneling amplitudes M and ΔM (taking this phase into account is simple,^{43–45} but makes the formalism significantly lengthier, see Appendix). For a given position x of the oscillator, the average detector current is $I_x = 2\pi |M + \Delta M x|^2 \rho_l \rho_r e^2 V / \hbar$, where V is the QPC voltage which may vary in time with frequency ω comparable to ω_0 , e is the electron charge, and $\rho_{l,r}$ are the densities of states in the electrodes.

We assume a weak response of the detector, $|I_x - I_{x'}| \ll |I_x + I_{x'}|$, and therefore the linear dependence of the detector current on the measured position

$$I_x = I_0 + kx, \quad (6)$$

neglecting effects of detector nonlinearity.⁴⁶ Also, we neglect the dependence on x of the detector current spectral density S_I which is assumed to be flat in the frequency range of interest. Because the voltage V varies in time, I_0 , k , I_x , and S_I also depend on time, that will be taken into account explicitly in the next section. Notice that the white noise S_I is an intrinsic detector noise, which is defined for a fixed voltage on a time scale much shorter than the time scale of voltage variations, while the long-time spectral density of the detector current is obviously affected by the voltage changes as well as by the oscillating signal from the nanoresonator.

To describe the dynamics of the continuous quantum measurement process, we apply the quantum Bayesian approach practically following the derivation⁴⁷ for the case of qubit measurement. We will have to use similar assumptions; in particular, for the validity of the Markovian approximation we assume that the internal dynamics of the detector is much faster than the oscillator dynamics (this requires $eV \gg \hbar\omega_0$), we also assume that detector current is quasicontinuous (which requires $I_0/e \gg \omega_0$ and even stronger inequality $k\Delta x_0/e \gg \omega_0$).

To start the derivation, we first neglect the nanoresonator evolution due to \mathcal{H}_0 , \mathcal{H}_{env} , and \mathcal{H}_{fb} (which will be added later) and assume constant detector voltage V (variations of V , slow on the time scale of detector dynamics, will be taken into account later just as a parameter variation). Similar to Ref. 47, the derivation of the Bayesian equations can be done in two ways: “informational” and “microscopic.” Let us start with informational derivation.

Since the operator of the QPC current commutes with \hat{x} , the detector current is insensitive to the off-diagonal matrix elements of the resonator density matrix $\rho(x, x')$ in x -representation. For a measurement duration τ long enough compared to the detector time scales \hbar/eV and e/I_0 (and short compared to the resonator evolution due to $\mathcal{H}_0 + \mathcal{H}_{\text{env}} + \mathcal{H}_{\text{fb}}$ so that it can be neglected), the probability distribution of the noisy detector current averaged over τ , $\bar{I} = (1/\tau) \int_0^\tau I(t') dt'$, is given by

$$P(\bar{I}, \tau) = \int P_x(\bar{I}, \tau) \rho(x, x, 0) dx, \quad (7)$$

where the third argument of ρ is time and $P_x(\bar{I}, \tau)$ is the probability distribution for \bar{I} in the case of the resonator at position x . Since $\tau \gg e/I_0$, this distribution is Gaussian,

$$P_x(\bar{I}, \tau) = (2\pi D_I)^{-1/2} \exp[-(\bar{I} - I_x)^2 / 2D_I], \quad (8)$$

where $D_I = S_I / 2\tau$ is the variance. Notice that \bar{I} is treated as a classical variable because detector decoherence time (which is on the order of \hbar/eV) is much shorter than τ .

Since classical and quantum dynamics are indistinguishable when off-diagonal matrix elements of ρ cannot affect the evolution, the diagonal matrix elements of ρ should sat-

isfy the classical evolution of conditional probability given by the Bayes formula:⁴⁸

$$\rho(x, x', \tau) = \frac{\rho(x, x, 0) P_{\bar{x}}(\bar{I}, \tau)}{\int \rho(\bar{x}, \bar{x}, 0) P_{\bar{x}}(\bar{I}, \tau) d\bar{x}}, \quad (9)$$

where \bar{I} is now a particular result of actual measurement (so the evolution of ρ is conditioned on the measurement result \bar{I}).

Classical Bayes formula cannot tell us anything about the evolution of the off-diagonal matrix elements $\rho(x, x')$. However, in the case of an ideal detector⁴⁷ (such as QPC) the evolution equation can be derived using the same trick as in Ref. 47 by comparing the ensemble-averaged density matrix elements²⁵ $\rho_{\text{av}}(x, x')$ with the upper bound for $|\rho_{\text{av}}(x, x')|$ derived from the Bayesian viewpoint. Let us start from the obvious inequality

$$|\rho(x, x', \tau)| \leq \sqrt{\rho(x, x, \tau) \rho(x', x', \tau)} \quad (10)$$

and take into account that for different members of the ensemble (different realizations of the measurement process) the value of \bar{I} is different, with distribution $P(\bar{I}, \tau)$ given by Eq. (7). Performing averaging over realizations and using obvious inequality $|\rho_{\text{av}}| \leq |\rho|_{\text{av}}$ we transform inequality (10) into the following:

$$|\rho_{\text{av}}(x, x', \tau)| \leq \int \sqrt{\rho(x, x, \tau) \rho(x', x', \tau)} P(\bar{I}, \tau) d\bar{I}.$$

The integration over \bar{I} can be performed explicitly using Eqs. (9) and (8), that finally leads to an upper bound for the off-diagonal matrix elements

$$|\rho_{\text{av}}(x, x', \tau)| \leq \sqrt{\rho(x, x, 0) \rho(x', x', 0)} e^{-(I_x - I_{x'})^2 \tau / 4S_I}. \quad (11)$$

Now let us compare this inequality with the result of conventional ensemble-averaged approach;⁴⁹ as shown by Mozyrsky and Martin, in the large- V limit the measurement by a low-transparency QPC leads to decoherence of the nanoresonator state as $\rho_{\text{av}}(x, x', \tau) = \rho(x, x', 0) \exp[-(I_x - I_{x'})^2 \tau / 4S_I]$. Since the exponential factor is the same as in (11), then for a pure initial state, $|\rho(x, x', 0)| = \sqrt{\rho(x, x, 0) \rho(x', x', 0)}$, inequality (11) actually reaches its upper bound, which is possible *only if* inequality (10) reaches its upper bound for *each* measurement result [if (10) is a strict inequality for at least some realizations of measurement, then averaging over realizations makes (11) a strict inequality]. This means that *a pure state of resonator remains pure in the process of measurement*, similar to the case of qubit measurement.⁴⁷ Notice that complete absence of decoherence in a particular realization of the measurement process is because the QPC is an ideal detector, while for the SET the remaining decoherence rate would not be zero.⁴⁷

Combining the equality in (10) with Eq. (9), we express it as

$$\rho(x, x', \tau) = \frac{\rho(x, x', 0) \sqrt{P_x(\bar{I}, \tau) P_{x'}(\bar{I}, \tau)}}{\int \rho(\bar{x}, \bar{x}, 0) P_{\bar{x}}(\bar{I}, \tau) d\bar{x}}. \quad (12)$$

We have neglected the possible phase factor $\exp(i\phi_m)$ because in our model $\phi_m = 0$ since in the derivation presented above ϕ_m cannot depend on \bar{I} (otherwise the upper bound would not be reached) and there is no phase in the ensemble-averaged result.²⁵ The absence of phase ϕ_m can also be proven directly using the microscopic model discussed below. Nevertheless, nonzero ϕ_m can be present in somewhat different models which include ‘‘asymmetry’’ of the detector coupling;⁴³ an example of such case is when there is a relative phase^{44–46} between M and ΔM in the Hamiltonian (4) and (5) (see Appendix).

So far we have proven Eq. (12) only for a pure initial state $\rho(x, x', 0)$. It is also easy to show its validity for a mixed state. Representing initial state as $\rho(0) = \sum_i P_i(0) \rho_i(0)$, where P_i are the probabilities of pure states $\rho_i(0)$, we apply a ‘‘double-Bayesian’’ procedure (as in Ref. 45) in which $P_i(\tau)$ is found via classical Bayes theorem while each $\rho_i(\tau)$ satisfies the quantum Bayes equation (12). Simple algebra shows that evolution of the mixed density matrix ρ is still described by Eq. (12).

Besides using the ‘‘informational’’ approach described above, Eq. (12) can also be obtained in a ‘‘microscopic’’ way. Similar to the derivation for the qubit measurement,⁴⁷ the evolution can be divided into the sequence of sufficiently short segments consisting of ‘‘conventional’’ evolution of the nanoresonator and detector, in which all the detector degrees of freedom are traced over, except the number n of electrons passed through the detector, so that the magnitude of interest is the combined density matrix $\rho_n(x, x', t)$. At the boundaries between the segments we collapse the number n according to the orthodox procedure:⁵⁰ the probability of a particular ‘‘realized’’ $n = n_0$ is equal to $\int \rho_{n_0}(x, x, t) dx$, and the corresponding density matrix after collapse is

$$\rho_n(x, x', t + 0) = \frac{\rho_{n_0}(x, x', t - 0) \delta_{n, n_0}}{\int \rho_{n_0}(\bar{x}, \bar{x}, t - 0) d\bar{x}}, \quad (13)$$

where δ_{n, n_0} is the Kronecker symbol. Applying this sequential collapse procedure to the conventional evolution of $\rho_n(x, x', t)$ described by Eq. (6) of Ref. 25, we can obtain our Eq. (12) if the resonator evolution due to $\mathcal{H}_0 + \mathcal{H}_{\text{env}} + \mathcal{H}_{\text{fb}}$ is neglected and the limit of large detector voltage is assumed.

The differential equation describing evolution of the resonator state due to measurement can be obtained by differentiating Eq. (12) over time τ at $\tau = 0$ and using Eq. (8) (because of the Markovian approximation, this can be done for arbitrary starting time t):

$$\begin{aligned} \dot{\rho}(x, x', t) = & \rho(x, x', t) S_I^{-1} \{ I(t) [I_x + I_{x'} - 2\langle I(t) \rangle] \\ & - [I_x^2 + I_{x'}^2 - 2\langle I^2(t) \rangle] / 2 \}, \end{aligned} \quad (14)$$

where we have introduced notations $\langle I(t) \rangle = \int I_x \rho(x, x, t) dx$

and $\langle I^2(t) \rangle = \int I_x^2 \rho(x, x, t) dx$, while Eq. (7) transforms into

$$I(t) = \langle I(t) \rangle + \xi(t), \quad (15)$$

where $\xi(t)$ is a white noise with spectral density S_I (as mentioned before, we neglect dependence of S_I on x). Notice that Eq. (14) actually does not require the current linearity (6) and formally coincides with the similar equation for the case of entangled qubits measured by an ideal detector,⁴⁵ if x is replaced by the index corresponding to the state of qubits. For the linear detector with response (6), Eq. (14) becomes

$$\begin{aligned} \dot{\rho}(x, x') = & \rho(x, x') S_I^{-1} \{ [I(t) - I_0] k(x + x' - 2\langle x \rangle) \\ & - (k^2/2)[x^2 + (x')^2 - 2\langle x^2 \rangle] \}, \end{aligned} \quad (16)$$

where $\langle x \rangle = \int x \rho(x, x) dx$, $\langle x^2 \rangle = \int x^2 \rho(x, x) dx$, and for brevity we do not show explicitly the time dependence of ρ .

Notice that Eq. (14) has been obtained by differentiating Eq. (12) over τ using the standard rules for derivatives (i.e., using only the first order in $d\tau$). Therefore Eqs. (14) and (16) are the stochastic equations in the so-called Stratonovich form which assumes “centered” definition of the derivative, $\dot{\rho}(t) \equiv \lim_{\tau \rightarrow 0} [\rho(t + \tau/2) - \rho(t - \tau/2)] / \tau$, and allows us to use standard calculus rules.⁵¹ For a nonlinear stochastic equation the calculus rules are quite different for another widely used definition of the “forward” derivative, $\dot{\rho}(t) \equiv \lim_{\tau \rightarrow 0} [\rho(t + \tau) - \rho(t)] / \tau$, which would lead to an equation in the so-called Itô form.⁵¹ Advantage of the Itô form is the simple averaging over the noise (while averaging in Stratonovich form is not trivial); this is the reason why Itô form is usually preferred by mathematicians, even though physical intuition works better in the Stratonovich form. Translation back and forth between two forms is often useful to solve a particular problem.

The rule of translation between the two forms is the following:⁵¹ for a system of equations $\dot{y}_i(t) = G_i(\mathbf{y}, t) + F_i(\mathbf{y}, t)\xi(t)$ in the Stratonovich form, the corresponding Itô equation is $\dot{y}_i(t) = G_i(\mathbf{y}, t) + F_i(\mathbf{y}, t)\xi(t) + (S_\xi/4)\sum_j [dF_j(\mathbf{y}, t)/dy_j] F_j(\mathbf{y}, t)$, where y_i are the components of the vector \mathbf{y} , G_i and F_i are arbitrary functions, and S_ξ is the spectral density of white noise $\xi(t)$. To apply this rule to our case, we replace index i by continuous set (x, x') and replace summation by integration; F_i and G_i are now functionals of $\mathbf{y} = \rho(x, x')$, and the derivatives are replaced by functional derivatives. Using this rule, Eq. (16) is translated into the Itô form as

$$\begin{aligned} \dot{\rho}(x, x') = & (k/S_I)(x + x' - 2\langle x \rangle)\rho(x, x')\xi(t) \\ & - (k^2/4S_I)(x - x')^2\rho(x, x'). \end{aligned} \quad (17)$$

This equation is similar to equations derived in many publications (e.g., in Refs. 30, 33, 52, and 53) for measurement of a mechanical oscillator. Notice that the last term in Eq. (17) does not describe decoherence in a particular realization of the measurement (recall that a pure state remains pure); however, it describes ensemble decoherence, since averaging over the measurement result (over noise ξ) is done in Itô form simply by setting $\xi=0$. This term can also be rewritten in a standard double-commutator form (see, e.g., Refs. 25, 30, 33, 49, and 53–56) since $(x - x')^2\rho(x, x') = [\hat{x}, [\hat{x}, \rho]]_{x, x'}$.

Equation (17) describes the evolution of the nanoresonator state due to measurement by the ideal detector (low-transparency QPC) described by the Hamiltonian (4) and (5). To extend the formalism to a nonideal detector (for example, RF-SET) we introduce its quantum efficiency (ideality) $\eta \leq 1$ similar to Ref. 47 and replace the decoherence factor $k^2/4S_I$ by $k^2/4S_I\eta$. Simply speaking, $1/\eta$ is the ratio between the product of output and back-action noises of the detector and its quantum-limited value.^{32,47,57} For example, $k^2/4S_I$ in Eq. (17) can be replaced by $k^2/4S_I\eta$ when an extra term $-\gamma_{cl}(x - x')^2\rho(x, x')$ is due to additional classical back-action noise from the detector or when the output noise of the detector contains an additional noise (see Ref. 45 and Appendix). Notice that finite temperature T of the low-transparency QPC detector also reduces the detector efficiency down to⁴⁷ $\eta = \tanh^2(eV/2T)$.

As the final step of our derivation, we add into Eq. (17) (modified by efficiency η) the evolution due to terms $\mathcal{H}_0 + \mathcal{H}_{\text{env}} + \mathcal{H}_{\text{fb}}$ of the Hamiltonian (1). Interaction with the thermal bath denoted by \mathcal{H}_{env} can be described by the standard Brownian motion master equation.⁵⁸ Assuming weak coupling (large Q -factor) and arbitrary temperature T , we add damping and diffusion terms^{30,59} $-(i\omega_0/2\hbar Q)[\hat{x}, \{\hat{p}, \rho\}_+] - (m\omega_0^2/2\hbar Q)\coth(\hbar\omega_0/2T)[\hat{x}, [\hat{x}, \rho]]$ into the equation for $\dot{\rho}$. Therefore, our final equation for the nanoresonator evolution is (in Itô form)

$$\begin{aligned} \dot{\rho}(x, x') = & \frac{-i}{\hbar} [\mathcal{H}_0 + \mathcal{H}_{\text{fb}}, \rho]_{x, x'} - \frac{i\omega_0}{2\hbar Q} [\hat{x}, \{\hat{p}, \rho\}_+]_{x, x'} \\ & - \left(\frac{k^2}{4S_I\eta} + \frac{m\omega_0^2}{2\hbar Q} \coth \frac{\hbar\omega_0}{2T} + \gamma_{\text{add}} \right) (x - x')^2 \rho(x, x') \\ & + \frac{k}{S_I} (x + x' - 2\langle x \rangle) \rho(x, x') \xi(t), \end{aligned} \quad (18)$$

in which the white noise $\xi(t)$ is related to the detector current $I(t)$ via Eq. (15) as $\xi(t) = I(t) - I_0 - k\langle x(t) \rangle$ and γ_{add} is introduced phenomenologically to take into account sources of additional dephasing, for example due to high-temperature electromagnetic fields penetrating into cryostat (we will mostly assume $\gamma_{\text{add}}=0$). The damping term can be written in the explicit form using substitution $[\hat{x}, \{\hat{p}, \rho\}_+]_{x, x'} = -i\hbar(x - x')(\partial/\partial x - \partial/\partial x')\rho(x, x')$. Notice that there is no damping term due to measurement (in contrast to the term due to Q -factor) because we treat the detector as a device with completely classical output and therefore detector voltage is very large while its unnormalized coupling is very weak; in other words, we assume that the nanoresonator energy is limited well below the effective temperature of detector (which is on the order of eV) by other effects (feedback and Q -factor).

III. MEASUREMENT MODULATION AND EQUATIONS FOR GAUSSIAN STATES

Periodic modulation of the QPC voltage $V=f(t)V_0$ (with frequency comparable to ω_0 and much smaller than eV/\hbar and I_0/e) leads to the corresponding modulation of the measurement parameters: $k=f(t)k_0$, $I_x=f(t)(I_{00}+k_0x)$, S_I

$=|f(t)|S_0$, so that the “measurement strength” k^2/S_I is modulated as $|f(t)|k_0^2/S_0$ [in general $f(t)$ may be negative]. In the case of RF-SET the voltage dependence of parameters is not trivial (also the modulation can be arranged using the gate voltage instead of the bias), but we still can define $f(t)$ as the modulation of the measurement strength from equation

$$k^2/S_I = |f(t)|k_0^2/S_0. \quad (19)$$

Quantum efficiency η in general can also be affected by the modulation, but for simplicity we assume it to be constant. (In reality, we expect decrease of η at smaller voltages because of contribution from voltage-independent noise sources. However, these contributions can crudely be taken into account via reduction of the Q -factor and, moreover, they are assumed to be sufficiently small; therefore the effect of imperfect efficiency η is mainly taken into account during the large- V fraction of the modulation period.)

Notice that the noise $\xi(t)$ in Eq. (18) has implicit time dependence because of modulated in time spectral density S_I . To remove this dependence we define the white noise

$$\xi_0(t) = \xi(t)\sqrt{S_0/S_I} \operatorname{sgn}[f(t)] \quad (20)$$

with time-independent spectral density S_0 . Then the last term in Eq. (18) can be written as $\sqrt{|f(t)|}(k_0/S_0)(x+x' - 2\langle x \rangle)\rho(x, x')\xi_0(t)$.

Somewhat similar to the case of qubit measurement,⁴⁷ we define the dimensionless (time-dependent) coupling as

$$C = \frac{\hbar k^2}{S_I m \omega_0^2} = |f(t)|C_0, \quad (21)$$

which can also be expressed as $C = 4/\omega_0 \tau_m$, where $\tau_m = 2S_I/(k\Delta x_0)^2$ is the “measurement” time which would be necessary to distinguish (with signal-to-noise ratio of 1) two position states separated by the ground state width Δx_0 . We will mainly consider the case of weak coupling, $C \ll 1$, which corresponds to a realistic experimental situation. As an example, C is on the order of 10^{-6} for the experimental parameters of Ref. 5.

In this paper we will consider two types of modulation with frequency ω : harmonic modulation with the relative modulation depth $A_{\text{mod}} = (f_{\text{max}} - f_{\text{min}})/f_{\text{max}}$, $0 \leq A_{\text{mod}} \leq 2$:

$$f(t) = 1 + \frac{A_{\text{mod}}}{2}(-1 + \cos \omega t) \quad (22)$$

and the square-wave (stroboscopic) modulation with pulse width δt and relative depth A_{mod} ,

$$f(t) = \begin{cases} 1, & |t - j \times 2\pi/\omega| \leq \delta t/2, \quad j = 1, 2, \dots \\ 1 - A_{\text{mod}}, & \text{otherwise.} \end{cases} \quad (23)$$

Notice that $|f(t)| \leq 1$, so C_0 corresponds to the maximum coupling. Since $f(t)$ reaches zero in both types of modulation at $A_{\text{mod}} \geq 1$ (we will mostly consider 100% modulation, $A_{\text{mod}} = 1$), the conditions $eV \gg \hbar\omega_0$ and $k\Delta x_0/e \gg \omega_0$ required for the Bayesian formalism are violated during a fraction of the modulation period. Nevertheless, we will still use Eq. (18) for the analysis, that can be justified in the following way. Surely, even at $V=0$ the detector actually interacts and so

damps and dephases the nanoresonator [see, e.g., Eq. (7) in Ref. 25 which has the voltage-independent damping term], that is neglected in the Bayesian formalism, while the Bayesian evolution rate is crudely proportional to the voltage V (its strength relative to the neglected damping is crudely $eV/\hbar\omega_0$ for the resonator energy on the order of $\hbar\omega_0$). Therefore, the Bayesian evolution during the whole modulation period is much more significant than the neglected damping in the case of sufficiently large maximum voltage V_0 and not too large oscillation amplitude (the “heating” is prevented by feedback; otherwise the model would be inconsistent at $Q = \infty$). The neglected contribution is expected to lead to a weak damping of the nanoresonator state and can crudely be taken into account as some reduction of the Q -factor. [Equating the voltage-independent term in Eq. (7) of Ref. 25 with the second term of our Eq. (18), we obtain an estimate $Q = 2eV_0/\hbar\omega_0 C_0$ which is on the order of 10^{10} for the experimental parameters of Ref. 5.] Obviously, significant QND effect for stroboscopic measurement requires very weak coupling of the nanoresonator to outside world during the “off” fraction of the modulation period.

Following Refs. 30, 33, 60, and 61, we assume that the oscillator state can be described as a Gaussian state. This assumption can be justified by the fact that a Gaussian state remains Gaussian in the process of continuous measurement⁶¹ (we have checked this statement for nonideal detectors including “asymmetric” detectors and for varying in time strength of measurement) and by the fact that the thermal state (natural initial condition) is Gaussian.⁵⁸ It is also known⁶⁰ that any initial pure state approaches a Gaussian state in a course of continuous measurement by an ideal detector. We have also checked that a mixture of Gaussian states evolves into a single Gaussian state due to measurement.

A Gaussian state is defined⁵⁸ as a state for which the Wigner function $W(x, p) \equiv (\pi\hbar)^{-1} \int \rho(x+x', x-x') \exp(-2ix'p/\hbar) dx'$ has a Gaussian form,

$$W(x, p) = \text{Norm} \times \exp(-\mathbf{B}^T \mathbf{D}^{-1} \mathbf{B}/2),$$

$$\mathbf{B} = \begin{pmatrix} x - \langle x \rangle \\ p - \langle p \rangle \end{pmatrix}, \quad \mathbf{D} = \begin{pmatrix} D_x & D_{xp} \\ D_{xp} & D_p \end{pmatrix},$$

with normalization factor $\text{Norm} = [2\pi(D_x D_p - D_{xp}^2)]^{-1/2}$. In x -representation the density matrix of this state is

$$\begin{aligned} \rho(x, x') &= \frac{1}{\sqrt{2\pi D_x}} \exp\left[-\frac{\left(\frac{x+x'}{2} - \langle x \rangle\right)^2}{2D_x}\right] \\ &\times \exp\left[-\frac{(x-x')^2 (D_x D_p - D_{xp}^2)}{8D_x \hbar^2/4}\right] \\ &\times \exp\left[i(x-x')\left(\frac{\langle p \rangle}{\hbar} + \left(\frac{x+x'}{2} - \langle x \rangle\right) \frac{D_{xp}}{\hbar D_x}\right)\right]. \end{aligned} \quad (24)$$

The Gaussian state is characterized by only five real parameters: average position $\langle x \rangle = \langle \hat{x} \rangle$ and momentum $\langle p \rangle = \langle \hat{p} \rangle$, their variances $D_x = \langle \hat{x}^2 \rangle - \langle \hat{x} \rangle^2$ and $D_p = \langle \hat{p}^2 \rangle - \langle \hat{p} \rangle^2$, and the

correlation $D_{xp} = \langle \hat{x}\hat{p} + \hat{p}\hat{x} \rangle / 2 - \langle \hat{x} \rangle \langle \hat{p} \rangle$. These parameters satisfy the generalized Heisenberg inequality⁶²

$$D_x D_p - D_{xp}^2 \geq \hbar^2/4, \quad (25)$$

which reaches the lower bound for the pure states. In particular, “coherent” states are the Gaussian states with $D_x = (\Delta x_0)^2$, $D_p = (\hbar/2\Delta x_0)^2$, and $D_{xp} = 0$.

For Gaussian states Eq. (18) significantly simplifies and transforms into the following set of equations:

$$\langle \dot{\hat{x}} \rangle = \frac{\langle p \rangle}{m} + \frac{2k_0}{S_0} |f(t)|^{1/2} D_x \xi_0(t), \quad (26)$$

$$\langle \dot{\hat{p}} \rangle = -m\omega_0^2 \langle x \rangle + \frac{2k_0}{S_0} |f(t)|^{1/2} D_{xp} \xi_0(t) - \frac{\omega_0}{Q} \langle p \rangle + \mathcal{F}, \quad (27)$$

$$\dot{D}_x = \frac{2}{m} D_{xp} - \frac{2k_0^2}{S_0} |f(t)| D_x^2, \quad (28)$$

$$\begin{aligned} \dot{D}_p = & -2m\omega_0^2 D_{xp} + \frac{k_0^2 \hbar^2}{2S_0 \eta} |f(t)| - \frac{2k_0^2}{S_0} |f(t)| D_{xp}^2 - \frac{2\omega_0}{Q} D_p \\ & + \frac{\hbar m \omega_0^2}{Q} \coth \frac{\hbar \omega_0}{2T} + 2\hbar^2 \gamma_{\text{add}}, \end{aligned} \quad (29)$$

$$\dot{D}_{xp} = \frac{D_p}{m} - m\omega_0^2 D_x - \frac{2k_0^2}{S_0} |f(t)| D_x D_{xp} - \frac{\omega_0}{Q} D_{xp}, \quad (30)$$

which practically coincide with the equations derived in Refs. 33 and 30 (see also Ref. 60), except for the time dependent $f(t)$. It is interesting to notice that while Eq. (18) is a nonlinear stochastic equation, for which the Stratonovich and Ito forms are significantly different, there is no such difference for Eqs. (26)–(30), so they can be treated as simple ordinary differential equations.

Notice that the equations for D_x , D_p , and D_{xp} do not depend on noise $\xi_0(t)$ and feedback force \mathcal{F} , and are decoupled from the remaining equations. Therefore the evolution of the “wave packet shape” is deterministic (full “shape” is characterized by D_x , D_p , and D_{xp} ; however, for x -domain we are interested in D_x only). In contrast, the evolution of the packet centers $\langle x \rangle$ and $\langle p \rangle$ (in x - and p -domains) is random and thus is different for different realizations. To characterize the ensemble distribution of $\langle x \rangle$ and $\langle p \rangle$, in Sec. V we will analyze the corresponding variances (over realizations) $D_{\langle x \rangle}$, $D_{\langle p \rangle}$, and $D_{\langle x \rangle \langle p \rangle}$. Since the total (unconditional, ensemble-averaged) x -width of the nanoresonator state is $\sqrt{D_x + D_{\langle x \rangle}}$, both x -variances should be made smaller than the ground state variance Δx_0^2 in order to produce the x -squeezed state. In the next section we will show that D_x may be made significantly smaller than Δx_0^2 using measurement modulation $f(t)$, while in Sec. V we will show that $D_{\langle x \rangle}$ can be made even smaller using feedback.

IV. WAVE PACKET WIDTH SQUEEZING

In this section we analyze Eqs. (28)–(30) and show that the x -width $\sqrt{D_x}$ of the nanoresonator wave packet can be made much smaller than $\Delta x_0 = \sqrt{\hbar/2m\omega_0}$. Let us use the natural normalization of D_x and D_p by the ground state parameters, $d_x \equiv D_x/(\hbar/2m\omega_0)$, $d_p \equiv D_p/(\hbar m\omega_0/2)$, and similarly $d_{xp} \equiv D_{xp}/(\hbar/2)$. Then Eqs. (28)–(30) can be rewritten as

$$\dot{d}_x/\omega_0 = 2d_{xp} - C_0 |f(t)| d_x^2, \quad (31)$$

$$\begin{aligned} \dot{d}_p/\omega_0 = & -2d_{xp} + (C_0/\eta) |f(t)| - C_0 |f(t)| d_{xp}^2 - \frac{2}{Q} d_p \\ & + \frac{2}{Q} \coth \frac{\hbar \omega_0}{2T} + \frac{4\hbar \gamma_{\text{add}}}{m\omega_0^2}, \end{aligned} \quad (32)$$

$$\dot{d}_{xp}/\omega_0 = d_p - d_x - C_0 |f(t)| d_x d_{xp} - \frac{1}{Q} d_{xp}. \quad (33)$$

It is easy to see that the effect of additional dephasing γ_{add} is equivalent (in case of finite Q -factor) to increase of environment temperature T ; so we will not consider this effect separately ($\gamma_{\text{add}}=0$ is assumed for the rest of the paper). Also, let us postpone the analysis of effects due to finite Q and temperature until Sec. IV D, and start with the case of infinite Q -factor.

A. Numerical results for squeezing degree \mathcal{S}

We have analyzed Eqs. (31)–(33) numerically for the harmonic (22) and stroboscopic (23) modulation $f(t)$ for several values of the maximum coupling C_0 , concentrating on the range $C_0 \leq 1$. Notice that for the stroboscopic modulation the evolution during each period of modulation can be calculated analytically using Riccati equations³³ that significantly simplifies the numerical calculations. As anticipated, we have found that irrespectively of the initial conditions, Eqs. (31)–(33) approach the asymptotic solutions which oscillate with the modulation frequency ω (Fig. 2). Even for small coupling, $C_0 \ll 1$, the asymptotic oscillations can be significant in the case of resonance: $\omega \approx 2\omega_0/n$ (notice that at $C_0 = 0$ the variances oscillate with frequency $2\omega_0$). During the oscillation period the asymptotic solution for $d_x(t)$ reaches the values both above and below the stationary solution for $f(t)=1$ which is^{30,33}

$$d_x = (\sqrt{2/C_0}) [(1 + C_0^2/\eta)^{1/2} - 1]^{1/2} \quad (34)$$

and becomes $d_x = 1/\sqrt{\eta}$ for $C_0 \ll 1$. Most importantly, the squeezed state, $d_x < 1$, can be achieved for both harmonic and stroboscopic modulation.

Figure 3 shows the x -squeezing maximized over the oscillation period for the asymptotic solution, $\mathcal{S} \equiv \max_t [1/d_x(t)] = \max_t [\Delta x_0^2/D_x(t)]$, as a function of the modulation frequency ω for the harmonic modulation (22) and several values of coupling C_0 , efficiency η and modulation amplitude A_{mod} . (Notice that in the rotating frame the squeezing \mathcal{S} does not depend on time for weak coupling.) One can see that maximum squeezing is achieved for modu-

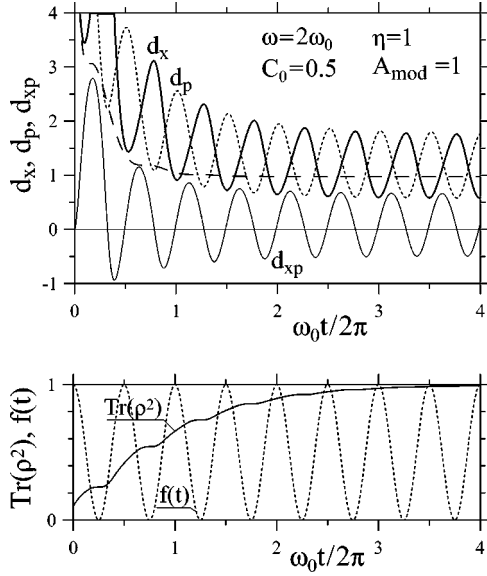


FIG. 2. An example of time dependence of dimensionless wave packet variances d_x , d_p , and d_{xp} (upper panel) for harmonic modulation $f(t)$ of measurement strength shown in the lower panel. After a transient period the evolution reaches stationary oscillating regime. The state purity $\text{Tr}(\rho^2)$ (lower panel) gradually approaches unity (mixed initial state with $d_x=d_p=10$ is chosen). The long-dashed line in the upper panel shows evolution of d_x in the non-modulated case $f(t)=1$.

lation with twice the resonator frequency, $\omega=2\omega_0$, 100% amplitude, $A_{\text{mod}}=1$, and for ideal detector, $\eta=1$. The value of maximum squeezing does not depend much on coupling C_0 [Fig. 3(a)] and is equal to $\mathcal{S} \approx 1.73$ for weak coupling, while the width of resonance scales proportionally to C_0 (analytical results discussed later and shown by dashed lines confirm this behavior). For nonideal detectors, $\eta < 1$ [Fig. 3(b)], the height of the peak decreases, $\mathcal{S}(2\omega_0) \approx 1.73\sqrt{\eta}$, and its width increases. Away from the resonance \mathcal{S} approaches the value for non-modulated measurement given by Eq. (34) [dotted lines in Fig. 3(b)]. Besides the main resonance, there are resonances at $\omega=2\omega_0/n$, $n \geq 2$, which are barely visible in Figs. 3(a) and 3(b) and lead to small shoulders rather than to peaks. However, these resonances become much better visible for modulation amplitudes A_{mod} greater than 100% as shown in Fig. 3(c). In particular, for $A_{\text{mod}}=2$ there is no peak at $\omega=2\omega_0$, and the main peak is at $\omega=\omega_0$; this is obviously because in this case $|f(t)|$ oscillates with frequency 2ω instead of ω .

Much stronger squeezing can be achieved for the stroboscopic modulation (23) of the measurement. Figure 4 shows $\mathcal{S}(\omega)$ for the ideal detector with $C_0=0.5$ and pulse duration $\delta t=0.05T_0$, where $T_0=2\pi/\omega_0$ is the nanoresonator period. One can see that as expected from the standard theory of stroboscopic QND measurements,^{12,13} there are sharp resonances at $\omega=2\omega_0/n$. In the case of full modulation, $A_{\text{mod}}=1$, shown in Fig. 4(a), the resonances have equal height; however, their width decreases with n . According to the QND idea, the squeezing should significantly decrease if measurement is not switched completely off between the measurement pulses. Comparing Figs. 4(a) and 4(b) we see

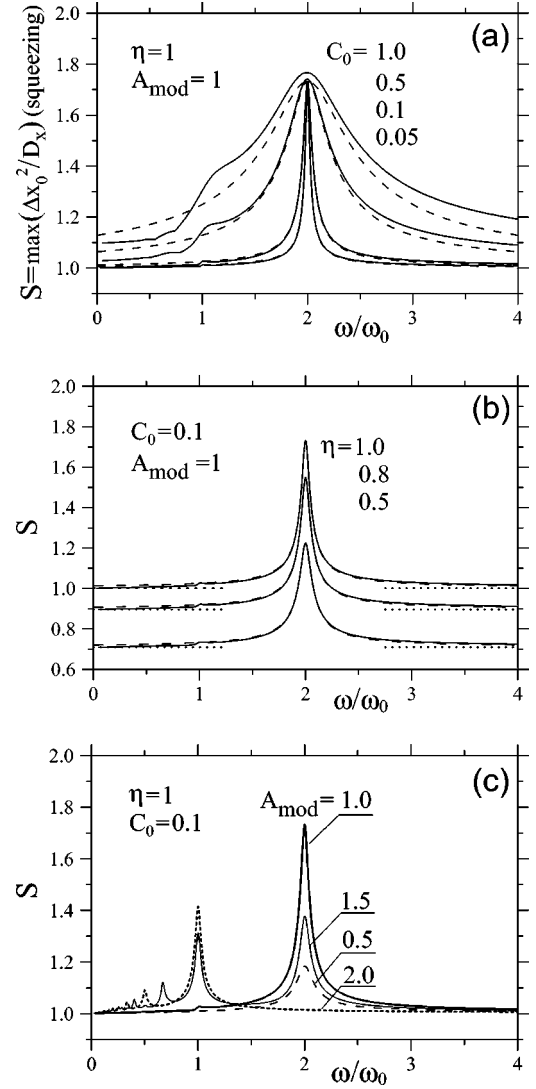


FIG. 3. Dependence of the packet width squeezing \mathcal{S} (maximized over the modulation period) on the frequency ω of the harmonic modulation (22) of the measurement strength, for several values of (a) the coupling C_0 , (b) detector quantum efficiency η , and (c) modulation amplitude A_{mod} . Solid lines in (a) and (b) are the numerical results while dashed lines are the analytical results corresponding to Eqs. (41) and (43); the dotted lines in (b) are the asymptotes $\mathcal{S}=\sqrt{\eta}$.

that the on/off ratio even as large as 10^3 leads to a considerable decrease of \mathcal{S} [obviously, the effect of finite on/off ratio becomes more important with decrease of $\delta t/T_0$]. Another consequence of finite on/off ratio is the decrease of the resonant peak height at $\omega=2\omega_0/n$ with n .

The results presented in Fig. 5(a) show that for smaller coupling C_0 the peak height remains practically the same, but the peak width decreases (this is the reason why we chose relatively large coupling in Fig. 4 in order to have a noticeable peak width). For smaller pulse duration δt , the squeezing peak becomes higher and narrower [Fig. 5(b)], while the detector nonideality makes the peak lower and wider [Fig. 5(c)]. All these dependencies will be confirmed by the analytical results discussed below and shown in Fig. 5 by dashed

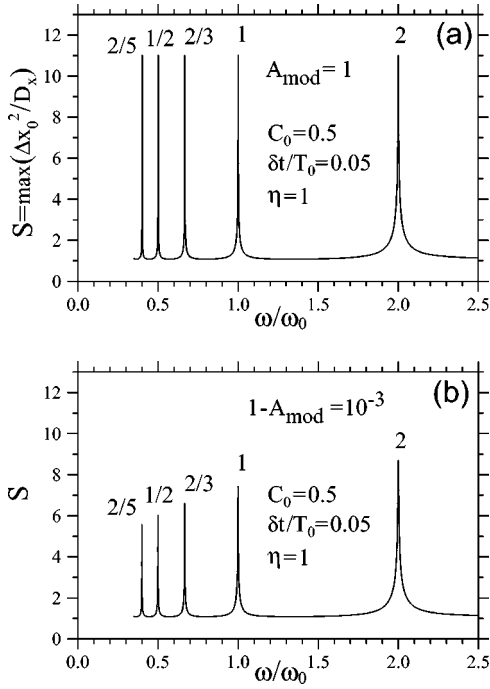


FIG. 4. Numerical results for the packet width squeezing S as a function of modulation frequency ω for the stroboscopic measurement modulation (23) with finite pulse duration δt . Efficient squeezing occurs at $\omega \approx 2\omega_0/n$. Infinitely large Q -factor of the nanoresonator is assumed.

and dotted lines (dashed lines show more accurate results while dotted lines correspond to a simpler formula).

B. Analytical results for squeezing S

1. Evolution of the state purity

Before discussing the analytical results for squeezing, let us briefly discuss the evolution of the state purity, $\text{Tr}(\rho^2) = (\hbar/2)/\sqrt{D_x D_p - D_{xp}^2} = 1/\sqrt{u}$, where $u \equiv d_x d_p - d_{xp}^2$. From Eqs. (31)–(33) (with $Q = \infty$ and $\gamma_{\text{add}} = 0$) it is easy to derive the equation

$$\dot{u} = \omega_0 C_0 |f(t)| d_x (\eta^{-1} - u). \quad (35)$$

Since C_0 and d_x are both positive, the asymptotic solution of this equation is obviously $u = 1/\eta$ and therefore the state purity reaches the asymptote $\text{Tr}(\rho^2) = \sqrt{\eta}$. In particular, in the case of ideal detector, $\eta = 1$, the state eventually becomes pure (similar to the case of a qubit measurement⁴⁷). As will be discussed later, the typical purification time is comparable to the time of reaching the asymptotic regime for variances d_x and d_p .

2. Analytics for harmonic modulation

For simplicity in this subsection we consider the harmonic modulation (22) of the measurement strength only with 100% modulation, $A_{\text{mod}} = 1$ (which leads to maximum squeezing), and we still assume $Q = \infty$. Without measurement, $C_0 = 0$, Eqs. (31)–(33) have the solution

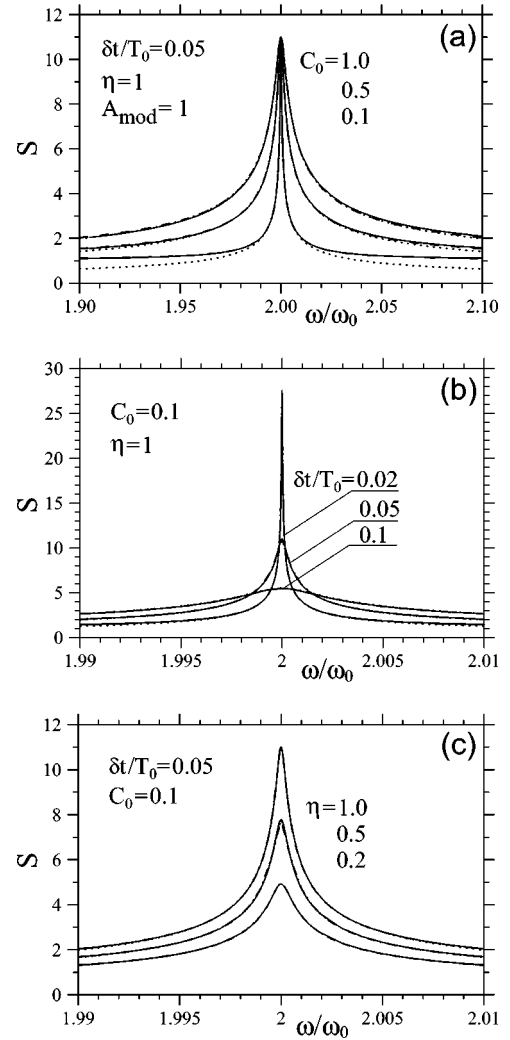


FIG. 5. The shape of the squeezing peak $S(\omega)$ at $\omega \approx 2\omega_0$ for stroboscopic modulation, for several values of (a) coupling with detector C_0 , (b) pulse duration δt ($T_0 = 2\pi/\omega_0$ is the resonator period), and (c) quantum efficiency of measurement η . Solid lines show numerical results, dashed lines (practically indistinguishable from the solid lines) are the analytical results given by Eqs. (49) and (41), and the dotted lines are calculated using the simplified equation (51). The height of the squeezing peak is proportional to $\sqrt{\eta/\delta t}$ [Eq. (52)] while its width is proportional to $C_0(\delta t)^3/n^2\sqrt{\eta}$ [Eq. (53)].

$$d_x(t) = \sqrt{\eta^{-1} + A^2} - A \cos(2\omega_0 t + \varphi), \quad (36)$$

$$d_p(t) = \sqrt{\eta^{-1} + A^2} + A \cos(2\omega_0 t + \varphi), \quad (37)$$

$$d_{xp}(t) = A \sin(2\omega_0 t + \varphi), \quad (38)$$

with arbitrary amplitude A and phase φ . (Notice that these equations satisfy the asymptotic condition $\text{Tr} \rho^2 = \sqrt{\eta}$.) For weak coupling, $C_0/\eta \ll 1$, and harmonic modulation (22) in the vicinity of the resonance, $\omega \approx 2\omega_0$, it is natural to look for the asymptotic solution of Eqs. (31)–(33) in the form (36)–(38) with $2\omega_0$ replaced by ω (actually, A and φ vary in

time with frequency ω , but variations are negligible at $C_0/\eta \ll 1$.

To find A and φ , we substitute these equations into the equation $\int_{-\pi/\omega}^{\pi/\omega} f(t)(\eta^{-1} - d_x^2 - d_{xp}^2)dt = 0$ which follows from the stationarity condition, $\int_{-\pi/\omega}^{\pi/\omega} (\dot{d}_x + \dot{d}_p)dt = 0$, and Eqs. (31) and (32). This gives us the relation

$$A = \frac{1}{2} \sqrt{\eta^{-1} + A^2} \cos \varphi. \quad (39)$$

We find numerically and analytically (see below) that $\varphi = 0$ at the resonance, $\omega = 2\omega_0$. (This is quite natural: smaller d_x correspond to larger measurement strength.) Then from Eq. (39) we find $A = 1/\sqrt{3}\eta$ and therefore

$$S(2\omega_0) = \sqrt{3}\eta \quad (40)$$

since the maximum squeezing S and the amplitude A are related as

$$S = \eta(A + \sqrt{A^2 + \eta^{-1}}). \quad (41)$$

This result confirms the numerical result for the peak height in Fig. 1.

To find the shape of the resonant peak, we need one more equation relating A and φ . It can be obtained by deriving equation for $\ddot{d}_{xp}(t)$ from Eqs. (31)–(33), and equating the $\sin(\omega t + \varphi)$ component for the two sides of the equation (assuming $C_0/\eta \ll 1$ and $\omega \approx 2\omega_0$). In this way we obtain

$$(4\omega_0^2 - \omega^2)A = \eta^{-1}C_0\omega_0^2 \sin \varphi. \quad (42)$$

In particular, this proves that $\varphi = 0$ at $\omega = 2\omega_0$. Combining Eqs. (39) and (42) we find the amplitude A as

$$A(\omega) = \sqrt{\frac{2/\eta}{3 + g(\omega) + \sqrt{g^2(\omega) + 10g(\omega) + 9}}}, \quad (43)$$

where $g(\omega) = 16\eta(2 - \omega/\omega_0)^2/C_0^2$. The corresponding analytical result for squeezing S is obtained via Eq. (41). This result is shown by the dashed lines in Figs. 3(a) and 3(b), which practically coincide with the solid lines representing the numerical results. Notice that the linewidth of the peak is proportional to $C_0/\sqrt{\eta}$; away from the resonance A decreases to zero, and S approaches $S = \sqrt{\eta}$, which is the same as for the case without modulation.³³ The analytical result for $S(\omega)$ works well for coupling C_0 up to approximately 0.3; for larger C_0 there is a noticeable difference from the numerical result as seen in Fig. 3(a). It is curious that rather complex shape of the resonance peak given by Eqs. (41) and (43) is quite close to the square root of the Lorentzian shape

$$S(\omega) \approx \sqrt{\eta} \left(1 + \frac{\sqrt{3} - 1}{\sqrt{1 + 3[(\omega - 2\omega_0)/\Delta\omega]^2}} \right) \quad (44)$$

with half-width at half-height $\Delta\omega \approx 0.63\omega_0 C_0/\sqrt{\eta}$.

3. Analytics for stroboscopic modulation

In the case of stroboscopic modulation (23) of the measurement strength (in this subsection we assume full modulation, $A_{\text{mod}} = 1$, and still neglect Q -factor), the variances d_x , d_p , and d_{xp} should follow Eqs. (36)–(38) during the “off”

phase of the modulation, while during the measurement pulse of duration δt the parameters A and φ slowly change (we again assume the weak coupling limit) in accordance with Eqs. (31)–(33). In particular, close to the n th resonant peak of Fig. 4(a), $\omega \approx 2\omega_0/n$, the phase φ should change during the pulse by the small amount

$$\delta\varphi = -2\omega_0(2\pi/\omega) + 2\pi n \approx \pi n^2(\omega/\omega_0 - 2/n) \quad (45)$$

in order to match $2\pi/\omega$ periodicity of the asymptotic solution with the periodicity of free oscillations (36)–(38). On the other hand, $\delta\varphi$ can be found from the equation

$$\dot{\varphi} = -4\omega_0 C_0 \eta^{-1} |f(t)| d_{xp} / [(d_p - d_x)^2 + 4d_{xp}^2] \quad (46)$$

which follows from Eqs. (31)–(33). Integrating Eq. (46) within the pulse interval $|t| \leq \delta t/2$ using Eqs. (36)–(38) in which A and φ are assumed constant, we obtain $\delta\varphi = -C_0 \sin(\omega_0 \delta t) / \eta A$. Combining this result with Eq. (45) we obtain an equation relating A and φ ,

$$\pi n^2 A(\omega/\omega_0 - 2/n) = \eta^{-1} C_0 \sin(\omega_0 \delta t) \sin \varphi. \quad (47)$$

To obtain one more equation for A and φ , we use the condition $\int_{-\delta t/2}^{\delta t/2} (\dot{d}_x + \dot{d}_p)dt = 0$. Expressing the derivative $\dot{d}_x + \dot{d}_p$ from Eqs. (31) and (32) and using Eqs. (36)–(38), we get the equation

$$A\omega_0 \delta t = \sqrt{\eta^{-1} + A^2} \sin(\omega_0 \delta t) \cos \varphi. \quad (48)$$

Equations (47) and (48) are sufficient to find A for the n th resonance, though the expression is quite long,

$$A^2(\omega) = \frac{2\eta^{-1} \sin^2(\omega_0 \delta t)}{B(\omega) + \sqrt{B^2(\omega) + 4\tilde{g}(\omega) \sin^2(\omega_0 \delta t)}}, \quad (49)$$

where $B(\omega) = \tilde{g}(\omega) + (\omega_0 \delta t)^2 - \sin^2(\omega_0 \delta t)$ and $\tilde{g}(\omega) = \pi^2 n^2 (2/n - \omega/\omega_0)^2 \eta / C_0^2$. The squeezing S is obtained from this result using Eq. (41). The corresponding analytical curves are plotted in Fig. 5 by the dashed lines which practically coincide with the numerical results shown by the solid lines. One can see that the analytics works well even for $C_0 = 1$, even though we assumed $C_0 \ll 1$ for the derivation.

The value of squeezing at $\omega = 2\omega_0/n$ (peak height) can be obtained from Eq. (49), but it is easier to use Eq. (48) with $\varphi = 0$ [which follows from Eq. (47)], that leads to the result

$$S(2\omega_0/n) = \sqrt{\eta} \sqrt{\frac{\omega_0 \delta t + \sin(\omega_0 \delta t)}{\omega_0 \delta t - \sin(\omega_0 \delta t)}}. \quad (50)$$

The analytical results simplify in the case of short pulses, $\delta t \leq T_0 = 2\pi/\omega_0$, then

$$A^2(\omega) = \frac{6/(\omega_0 \delta t)^2 \eta}{1 + \sqrt{1 + \left[\frac{6\pi\sqrt{\eta} n^2 (\omega - 2\omega_0/n)}{C_0 (\delta t)^3 \omega_0^4} \right]^2}}, \quad (51)$$

which corresponds to the peak squeezing

$$S(2\omega_0/n) = 2\sqrt{3}\eta/\omega_0 \delta t \quad (52)$$

(since $S = 2\eta A$ for $S \gg 1$, and $A = \sqrt{3}/\omega_0 \delta t \sqrt{\eta}$), while the half-width at half-height of $S(\omega)$ is

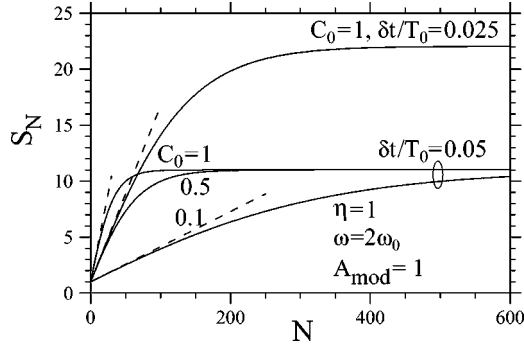


FIG. 6. Gradual buildup of squeezing S with number of measurement pulses N starting from the ground state for several values of coupling C_0 and pulse duration δt . Solid lines are the numerical results, dashed lines correspond to Eq. (54).

$$\Delta\omega = 2C_0(\delta t)^3\omega_0^4/\pi n^2\sqrt{3\eta}. \quad (53)$$

The curves calculated using Eq. (51) are shown in Fig. 5 by the dotted lines. There is a noticeable difference from the numerical results away from the resonance; however, the main part of the peak is fitted quite well.

Notice that in the case of exact resonance, $\omega = 2\omega_0/n$, the smallest x -width of the wavepacket is achieved at the middle of the measurement pulse, and at this point $d_x = 1/S$. However, d_x increases considerably even within the duration of the pulse, so that the maximum value $d_{x,\max}^{\delta t} = 4/S$ within the pulse is at its onset and end, while d_x averaged over the pulse duration is $\bar{d}_x^{\delta t} = 2/S$.

C. Time scale of squeezing buildup

An important question is how fast the squeezing approaches its asymptotic value calculated in Secs. IV A and IV B. In this subsection we analyze the duration of the transient period of squeezing buildup (see Fig. 2) for stroboscopic modulation $f(t)$ with $A_{\text{mod}} = 1$ and $\delta t/T_0 \ll 1$ at resonance, $\omega = 2\omega_0/n$, assuming $Q = \infty$.

Let us start with the standard QND case of instantaneous imprecise measurements,^{12,13} which corresponds to the formal limit $\delta t \rightarrow 0$, $C_0 \rightarrow \infty$, while $C_0\delta t = \text{const}$. Each measurement changes the resonator density matrix by multiplying it by a Gaussian function [see Eqs. (12) and (8)] with x -variance $D = (\Delta x_0)^2/C_0\omega_0\delta t$. Since the free resonator evolution in between the measurements can be neglected if the measurements are separated by integer number of half-periods, the total strength of repeated measurements adds up (product of two Gaussians is a Gaussian with added inverse variances). Therefore for a Gaussian initial state (24) the squeezing magnitude S_N after N measurements is

$$S_N = NC_0\omega_0\delta t + S_0. \quad (54)$$

While for instantaneous measurements the magnitude of squeezing accumulates indefinitely, for a continuous stroboscopic measurement with finite δt the quantum back-action cannot be avoided completely, so the squeezing increases as Eq. (54) only during the initial transient period (Fig. 6) and then saturates at the asymptotic level analyzed in Secs. IV A

and IV B. Comparing the asymptotic value S_∞ given by Eq. (52) with the linear increase from Eq. (54) and neglecting initial value S_0 , we obtain the estimate

$$N_b = \frac{2\sqrt{3}\eta}{C_0(\omega_0\delta t)^2} \quad (55)$$

for the number of measurement pulses necessary for almost complete buildup of squeezing (of course the numerical factor $2\sqrt{3}$ is not really important here).

Since the saturation of S_N is a gradual process, let us also analyze analytically the N -dependence for $N \geq N_b$ when S_N is already close to S_∞ . Let us start with Eqs. (36)–(38) assuming that the asymptotic purity $\text{Tr}(\rho^2) = \sqrt{\eta}$ is already reached but the parameter A still changes with N . Following the derivation used in Sec. IV B 3, we combine Eqs. (36) and (37) with (31) and (32) and obtain $\dot{d}_x + \dot{d}_p = 2A\dot{A}/\sqrt{\eta^{-1} + A^2} = \omega_0 C_0 |f(t)| (\eta^{-1} - d_x^2 - d_{xp}^2)$. Integrating this equation over the measurement pulse duration (assuming $C_0 \ll 1$ and $\varphi = 0$) we find the corresponding small change of the parameter A :

$$\frac{\Delta A}{\Delta N} = C_0 \sqrt{\eta^{-1} + A^2} [\sqrt{\eta^{-1} + A^2} \sin \omega_0 \delta t - A \omega_0 \delta t].$$

Translating this equation into evolution of squeezing and assuming $|S_N - S_\infty| \ll S_\infty$, $\omega_0 \delta t \ll 1$, $A^2 \gg \eta^{-1}$, we obtain

$$\frac{\Delta S_N}{\Delta N} = -\frac{C_0(\omega_0\delta t)^2}{\sqrt{3}\eta}(S_N - S_\infty), \quad (56)$$

which shows the exponential approach of the squeezing S_N towards S_∞ as $\exp(-2N/N_b)$, i.e. the typical number of measurements necessary to reach the asymptotic value is similar to what was found from initial part of the transient, Eq. (55).

It is interesting to notice that the time scale of the purity factor saturation (see Fig. 2) is similar to the time scale of squeezing saturation. Using Eq. (35) for $u \equiv d_x d_p - d_{xp}^2 = 1/\text{Tr}^2(\rho^2)$ and approximating average d_x within the pulse duration as $\bar{d}_x^{\delta t} = [1/\eta A + A(\omega_0\delta t)^2/4]/2$, which becomes $\bar{d}_x^{\delta t} \approx 2/S_\infty$ close to saturation, we obtain

$$\frac{\Delta u}{\Delta N} = -\frac{C_0(\omega_0\delta t)^2}{\sqrt{3}\eta}(u - 1/\eta). \quad (57)$$

Therefore, similar to S_N behavior, u also approaches asymptote as $\exp(-2N/N_b)$. Far from saturation we expect $\bar{d}_x^{\delta t} > 2/S_\infty$, and therefore a larger initial rate of reaching the asymptote.

Finite time scale of squeezing buildup is important if an allowed experimental “waiting time” τ_w is limited. Figure 7 shows the squeezing S as a function of measurement pulse duration δt for several values of τ_w (initial state is chosen to be the ground state). While the upper line ($\tau_w = \infty$) corresponds to Eq. (52) and increases indefinitely at small δt , the squeezing for finite waiting time τ_w reaches maximum at an optimum pulse duration δt . For smaller δt the squeezing buildup is too slow [see Eq. (55)] and the squeezing is limited by the accumulated measurement strength $C_0(2\tau_w/T_0)(\delta t/T_0)$, while for larger δt the limiting factor is too strong back-action.

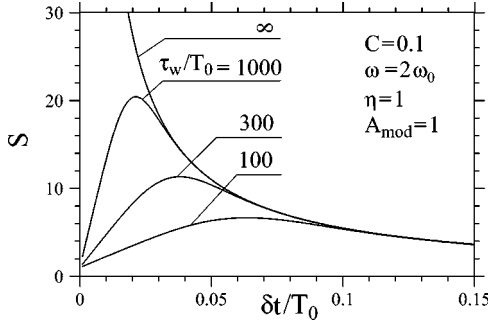


FIG. 7. Squeezing \mathcal{S} as a function of the pulse duration δt for stroboscopic measurements with a particular “waiting time” τ_w allowed for squeezing buildup.

Numerical calculations show that this maximum squeezing is fitted well by the formula

$$\mathcal{S}_{\max} \approx 2.0 \sqrt{C_0 \tau_w / T_0} \quad (\omega = 2\omega_0, \eta = 1). \quad (58)$$

[For example, this fitting formula underestimates the numerical results for $C_0=0.1$ ($C_0=0.5$) by 9% (4.6%) for $\tau_{\text{wait}}/T_0=30$ and by 2.2% (1.2%) for $\tau_{\text{wait}}/T_0=1000$.]

For an analytical estimate of \mathcal{S}_{\max} let us assume that optimum δt corresponds to the condition of squeezing buildup time being comparable to the waiting time, $2\tau_w/T_0 \approx N_b$ [see Eq. (55)]. Then the optimum is achieved at

$$\delta t_{\text{opt}}/T_0 \approx 0.21 \eta^{1/4} / (C_0 \tau_w / T_0)^{1/2} \quad (59)$$

(which is well confirmed by results in Fig. 7) and the corresponding \mathcal{S}_{\max} calculated from Eq. (52) is

$$\mathcal{S}_{\max} \approx 2(3\eta)^{1/4} \sqrt{C_0 \tau_w / T_0}, \quad (60)$$

which differs from the numerical result (58) only by a factor ≈ 1.3 .

It is tempting to guess that the effect of finite Q -factor (at least for zero temperature of environment) can be described by a similar formula with τ_w replaced by QT_0 (so that $\mathcal{S}_{\max} \approx \eta^{1/4} \sqrt{C_0 Q}$) since τ_w is naturally restricted by the resonator damping time. However, as will be seen in the next section, this gives only an upper bound and finite Q -factor actually leads to a significantly smaller value of \mathcal{S}_{\max} .

D. Effects of finite Q -factor and environment temperature

In this section we analyze effects of finite quality factor Q of the nanoresonator and environment temperature T for stroboscopic measurement with $\omega = 2\omega_0/n$ and $A_{\text{mod}} = 1$. (Extra dephasing γ_{add} is equivalent to increase of T .)

Numerical solution of Eqs. (31)–(33) with a finite Q -factor ($Q \gg 1$) shows that as expected the squeezing \mathcal{S} decreases at sufficiently small Q , and higher temperature also decreases \mathcal{S} . While for $Q = \infty$ the squeezing does not depend on coupling with detector $C_0 \leq 1$ for a fixed pulse duration δt [see Fig. 5(a) and Eq. (52)], for a finite Q the squeezing starts to decrease for too small C_0 , since coupling with detector competes with coupling to environment. [The effect is to some extent similar to the effect of $A_{\text{mod}} < 1$; in particular, the squeezing at $\omega = 2\omega_0/n$ decreases stronger with n as in

Fig. 4(b).] Notice that for infinite Q the environment temperature is not important since nanoresonator is not coupled to the environment and the evolution is determined by coupling with detector only.

For an analytical analysis let us mention first that the asymptotic purity $\text{Tr}(\rho^2) = 1/\sqrt{u}$ is no longer equal to $\sqrt{\eta}$, since Eq. (35) should be replaced by

$$\frac{\dot{u}}{\omega_0} = C_0 |f(t)| d_x (\eta^{-1} - u) - \frac{2u}{Q} + \frac{2d_x}{Q} \coth \frac{\hbar\omega_0}{2T}. \quad (61)$$

For $Q \gg 1$ we can neglect small asymptotic oscillations of u and assume a practically constant asymptotic value \bar{u} . Since the average of Eq. (61) over the oscillation period should be equal to zero in the asymptotic regime, we can find \bar{u} from equation

$$C_0 \overline{d_x^{\delta t}} \frac{\omega \delta t}{2\pi} (\eta^{-1} - \bar{u}) - \frac{2}{Q} \left(\bar{u} - \overline{d_x} \coth \frac{\hbar\omega_0}{2T} \right) = 0, \quad (62)$$

where $\overline{d_x^{\delta t}}$ is d_x averaged over the pulse duration while $\overline{d_x}$ is averaged over the whole period.

To find $\overline{d_x^{\delta t}}$ and $\overline{d_x}$ we use Eqs. (36)–(38) which are still applicable for the asymptotic oscillations of d_x , d_p , and d_{xp} if η^{-1} in these equations is replaced with \bar{u} . Still assuming no phase shift φ in the case of exact resonance $\omega = 2\omega_0/n$ (this has been confirmed numerically), we obtain

$$(\eta^{-1} - \bar{u}) [\sqrt{\bar{u} + A^2} \omega_0 \delta t - A \sin(\omega_0 \delta t)] + (2\pi n / C_0 Q) \times [\coth(\hbar\omega_0/2T) \sqrt{\bar{u} + A^2} - \bar{u}] = 0. \quad (63)$$

One more equation which relates \bar{u} and A follows from zero average of $\dot{d}_x + \dot{d}_p$ in the stationary regime. Using Eqs. (31)–(33) and modified Eqs. (36)–(38) we find

$$(\eta^{-1} - 2A^2 - \bar{u}) \omega_0 \delta t + 2A \sqrt{\bar{u} + A^2} \sin(\omega_0 \delta t) - (2\pi n / C_0 Q) \times [\sqrt{\bar{u} + A^2} - \coth(\hbar\omega_0/2T)] = 0. \quad (64)$$

We have checked that the squeezing $\mathcal{S} = (A + \sqrt{A^2 + \bar{u}}) / \bar{u}$ [see Eq. (41)] calculated from the numerical solution of Eqs. (63) and (64) practically coincides with results from direct solution of Eqs. (31)–(33) for $C_0 Q \geq 10$. It is also easy to check that in the limit $Q = \infty$ Eq. (64) transforms into Eq. (48); therefore we reproduce our previous results (50) and (52) for squeezing.

Solid lines in Fig. 8 show the dependence of maximum squeezing (optimized over the pulse duration δt) as a function of the product $C_0 Q$ for several temperatures of the environment, calculated numerically using Eqs. (63) and (64) for $\omega = 2\omega_0$. These results are fitted well by the formula

$$\mathcal{S}_{\max} = \frac{3}{4} \left[\frac{\sqrt{\eta} C_0 Q}{\coth(\hbar\omega_0/2T)} \right]^{1/3}, \quad (65)$$

shown by dashed lines in Fig. 8. As we see, the scaling $(C_0 Q)^{1/3}$ is more restrictive than scaling $(C_0 Q)^{1/2}$ which could be guessed from Eq. (60).

For an analytical estimate of \mathcal{S}_{\max} let us start with high-temperature case, $T \gg \hbar\omega_0$. The thermal noise contributes to the increase of x -variance (due to random walk) crudely as⁸

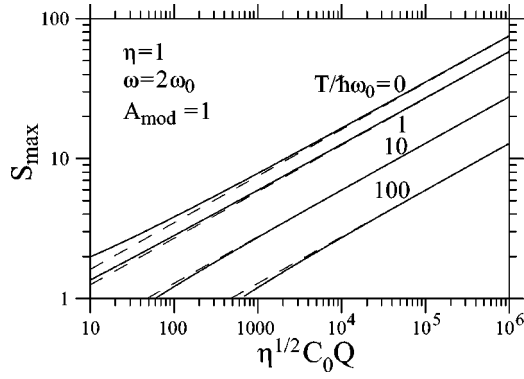


FIG. 8. The squeezing \mathcal{S} maximized over the stroboscopic pulse duration δt as a function of nanostructure Q -factor (multiplied by coupling with detector C_0 and square root of efficiency η) for several values of nanostructure temperature T . Solid lines are the numerical results, dashed lines correspond to the fitting formula (65).

$\dot{d}_x = (2T/\hbar\omega_0)(\omega_0/Q)$. In stationary state this increase is compensated by the squeezing buildup contribution which can be estimated from Eq. (54) as $\dot{d}_x = -(2/nT_0)C_0\omega_0\delta t/S^2$, assuming that \mathcal{S} is mainly limited by the effect of Q -factor [so \mathcal{S} is much smaller than the value given by Eq. (52) for infinite Q]. Equating two contributions, we obtain $\mathcal{S}^2 = (2/n) \times (\delta t/T_0)C_0Q(\hbar\omega_0/2T)$. Addition of quantum noise to the thermal noise leads to replacement of $2T/\hbar\omega_0$ by $\coth(\hbar\omega_0/2T)$, which gives

$$\mathcal{S} = \left[\frac{2\omega_0\delta t}{n} \frac{C_0Q}{2\pi \coth(\hbar\omega_0/2T)} \right]^{1/2}. \quad (66)$$

We have checked that numerical solutions of Eqs. (63) and (64) practically coincide with this formula when squeezing $\mathcal{S} \gg 1$ is mainly limited by Q -factor. Finally, comparing this formula with the limitation for infinite Q [Eq. (52)] and optimizing over δt , we obtain the estimate $\mathcal{S}_{\max} = a[\sqrt{\eta}C_0Q/n \coth(\hbar\omega_0/2T)]^{1/3}$ confirming the fitting formula (65), with the numerical factor $a \approx 1.03$; this factor is obviously supposed to overestimate the result of numerical optimization, Eq. (65).

As follows from Eqs. (65), (66), and (52), the effect of finite Q -factor is not important only when both C_0Q and $C_0Q\hbar\omega_0/T$ are much larger than $\mathcal{S}^3/\sqrt{\eta} \sim \eta/(\omega_0\delta t)^3$.

V. QUANTUM FEEDBACK OF THE PACKET CENTER

As shown in the previous section, the x -width of the monitored Gaussian wave packet can be squeezed well below the ground state width by applying periodic modulation $|f(t)|$ of the measurement strength. However, because of the measurement back-action, the center of the wave packet undergoes random evolution described by Eqs. (26) and (27), and without feedback diffuses far away from the origin. The diffusion is eventually limited either by damping due to finite Q -factor or by very large (formally infinite in our model) effective temperature (voltage) of the detector.^{25,30,33} Even though the evolution of the wave packet center can be monitored using Eqs. (26) and (27) in each realization of the

process and therefore the produced squeezed state is in principle useful for applications, large fluctuations of the center position would clearly lead to technical difficulties. The goal of this section is to show that the wavepacket center can be kept very close to origin all the time using quantum feedback.

The feedback is described by the force \mathcal{F} in Eq. (27). Similar to Refs. 33 and 30 we choose the linear feedback of the form

$$\mathcal{F} = -m\omega_0\gamma_x\langle x \rangle - \gamma_p\langle p \rangle, \quad (67)$$

where $\langle x \rangle$ and $\langle p \rangle$ are the continuously monitored values. To analyze the feedback performance we characterize^{30,33} the distribution of the packet center position $\langle x \rangle$ and center momentum $\langle p \rangle$ by the ensemble averages (over realizations) $\langle\langle x \rangle\rangle$ and $\langle\langle p \rangle\rangle$ and the variances $D_{\langle x \rangle} = \langle\langle x^2 \rangle\rangle - \langle\langle x \rangle\rangle^2$, $D_{\langle p \rangle} = \langle\langle p^2 \rangle\rangle - \langle\langle p \rangle\rangle^2$, $D_{\langle x \rangle \langle p \rangle} = \langle\langle x \rangle \langle p \rangle \rangle - \langle\langle x \rangle \rangle \langle\langle p \rangle \rangle$. In the notation of doubled angle brackets the inner brackets mean averaging with the density matrix ρ in an individual realization of the process, while the outer brackets is averaging over realizations. Notice that a natural characteristic of the total x -deviation of the state from the origin is the sum $D_x + D_{\langle x \rangle} + \langle\langle x \rangle\rangle^2$, so the feedback goal is to ensure $D_{\langle x \rangle} + \langle\langle x \rangle\rangle^2 \leq D_x = (\Delta x_0)^2/\mathcal{S}$ to keep the squeezed state sufficiently well centered.

The equations for $\langle\langle \dot{x} \rangle\rangle$ and $\langle\langle \dot{p} \rangle\rangle$ derived from Eqs. (26) and (27) lead to the ensemble-averaged evolution

$$\langle\langle \ddot{x} \rangle\rangle + (\gamma_p + \omega_0/Q)\langle\langle \dot{x} \rangle\rangle + (\omega_0^2 + \gamma_x\omega_0)\langle\langle x \rangle\rangle = 0, \quad (68)$$

which shows that $\langle\langle x \rangle\rangle$ eventually relaxes to zero for positive γ_p even if Q -factor is infinite.

Introducing dimensionless variances $d_{\langle x \rangle} \equiv D_{\langle x \rangle}2m\omega_0/\hbar$, $d_{\langle p \rangle} \equiv D_{\langle p \rangle}2/\hbar m\omega_0$, and $d_{\langle x \rangle \langle p \rangle} \equiv D_{\langle x \rangle \langle p \rangle}2/\hbar$, we derive^{30,33} the following equations from Eqs. (26) and (27):

$$\dot{d}_{\langle x \rangle}/\omega_0 = 2d_{\langle x \rangle \langle p \rangle} + C_0|f(t)|d_x^2, \quad (69)$$

$$\begin{aligned} \dot{d}_{\langle p \rangle}/\omega_0 = & -2d_{\langle x \rangle \langle p \rangle} - 2\mu F d_{\langle x \rangle \langle p \rangle} - 2F d_{\langle p \rangle} + C_0|f(t)|d_{xp}^2 \\ & - (2/Q)d_{\langle p \rangle}, \end{aligned} \quad (70)$$

$$\begin{aligned} \dot{d}_{\langle x \rangle \langle p \rangle}/\omega_0 = & d_{\langle p \rangle} - d_{\langle x \rangle} - \mu F d_{\langle x \rangle} - F d_{\langle x \rangle \langle p \rangle} + C_0|f(t)|d_x d_{xp} \\ & - (1/Q)d_{\langle x \rangle \langle p \rangle}, \end{aligned} \quad (71)$$

where $F = \gamma_p/\omega_0$ and $\mu = \gamma_x/\gamma_p$ are the dimensionless feedback parameters.

We have simulated these equations numerically using the asymptotic solutions of Eqs. (31)–(33) for d_x , d_p , and d_{xp} . We have mostly studied the resonance $\omega = 2\omega_0$ in the weakly coupling regime. Since finite Q -factor helps to decrease fluctuations of $\langle x \rangle$, we have considered only the case $Q = \infty$. The main finding is that for both harmonic and stroboscopic modulation of measurement, the center position variance $d_{\langle x \rangle}$ can be made much smaller than the packet variance d_x at time moments $t = j2\pi/\omega$ (j is integer) when the packet squeezing is at its maximum.

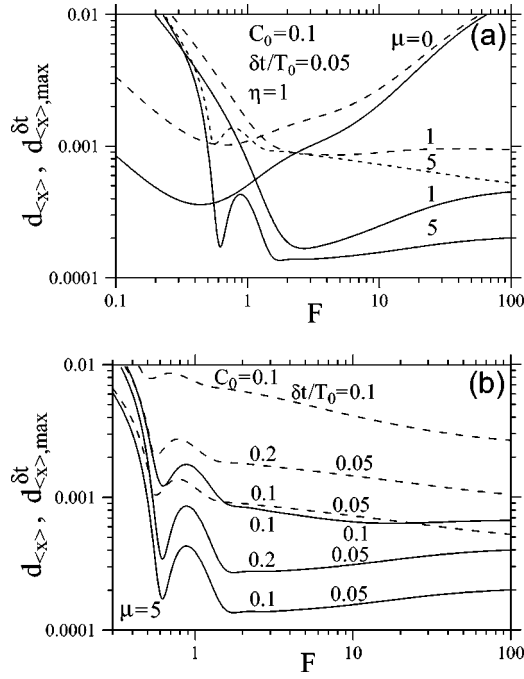


FIG. 9. Variance of the wave packet center $d_{(x)}$ at the middle of the stroboscopic measurement pulse (solid lines) and the variance $d_{(x),\max}^{\delta t}$ maximized over the pulse duration (dashed lines), as functions of feedback parameter F for several values of (a) feedback parameter μ and (b) parameters C_0 and δt . We assume $Q=\infty$, $\eta=1$, $\omega=2\omega_0$, and $A_{\text{mod}}=1$.

Solid lines in Fig. 9(a) show stationary values of $d_{(x)}$ at the center of the stroboscopic pulses, as function of the feedback factor F and several values of feedback factor μ . The chosen pulse duration $\delta t=0.05T_0$ corresponds to $d_x=1/S=0.091$, while the results for $d_{(x)}$ shown in Fig. 9(a) are much smaller. One can see that the feedback can operate sufficiently well even for $\mu=0$, so the term with γ_x in Eq. (67) is not really necessary; however, nonzero μ is beneficial since it leads to even smaller $d_{(x)}$. The curves in Fig. 9(a) saturate at $F\rightarrow\infty$, and the saturation value of $d_{(x)}$ decreases with increase of μ .

Solid lines in Fig. 9(b) show the dependence $d_{(x)}(F)$ for a fixed value $\mu=5$ and several values of the pulse duration δt and coupling C_0 . One can see that $d_{(x)}$ decreases with decrease of both δt and C_0 . Since d_x does not depend on C_0 [see Eq. (52)], the ratio $d_{(x)}/d_x$ obviously decreases at small coupling.

The packet center variance $d_{(x)}(t)$ changes significantly within the pulse duration; however, typically it is still much smaller than $1/S$. Dashed lines in Figs. 9(a) and 9(b) show $d_{(x)}$ maximized over the pulse duration (the maximum $d_{(x),\max}^{\delta t}$ is achieved at the end of pulse). The dependence of $d_{(x),\max}^{\delta t}$ on F , μ , δt , and C_0 is generally similar to the behavior of $d_{(x)}$ at the pulse center, though the values are several times higher.

For an analytical estimate of $d_{(x)}$ let us assume $F\gg 1$ and $\mu\geq 1$ (we also assume $C_0\ll 1$ and $\delta t/T_0\ll 1$). Because of the strong damping terms in Eqs. (69)–(71), the variances $d_{(x)}$,

$d_{(p)}$, and $d_{(x)(p)}$ decay practically to zero before the start of the measurement pulse. Within the pulse duration $d_{(x)(p)}$ can be found from Eq. (71) as $d_{(x)(p)}\approx -\mu d_{(x)}$. Substituting this value into Eq. (69) and using initial condition $d_{(x)}(-\delta t/2)=0$ at the beginning of the pulse, we obtain $d_{(x)}(t)=\omega_0 C_0 \int_{-\delta t/2}^t d_x^2(\tau) \exp[-2\mu\omega_0(t-\tau)] d\tau$. Now using the stationary solution $d_x(t)\approx S^{-1}+(\omega_0 t)^2 S/\eta$ which follows from Eq. (36) for $\varphi=0$ and $S\gg 1$, we can calculate the variance $d_{(x)}$ at the pulse center ($t=0$):

$$d_{(x)} = \frac{C_0(\omega_0\delta t)^3}{12\eta} \int_0^{1/2} (1+12y^2)^2 \exp[-2\mu y\omega_0\delta t] dy. \quad (72)$$

In the case $\mu\omega_0\delta t\gg 1$ this expression simplifies to

$$d_{(x)} = C_0(\omega_0\delta t)^2/24\mu\eta, \quad (73)$$

while in the opposite case $\mu\omega_0\delta t\ll 1$ it gives

$$d_{(x)} = C_0(\omega_0\delta t)^3/5\eta. \quad (74)$$

In both cases $d_{(x)}$ is much smaller than $S^{-1}=\omega_0\delta t/2\sqrt{3}\eta$ [see Eq. (52)] for small $\omega_0\delta t$ and/or small $C_0/\sqrt{\eta}$.

It is easy to see that the maximum value of $d_{(x)}(t)$ within the pulse duration is achieved at its end ($t=\delta t/2$), and can be calculated by Eq. (72) with the lower integration limit extended to $y=-1/2$ and with extra factor $\exp(-\mu\omega_0\delta t)$. In particular, this gives $d_{(x),\max}^{\delta t}=16d_{(x)}$ for $\mu\omega_0\delta t\gg 1$ and $d_{(x),\max}^{\delta t}=2d_{(x)}$ for $\mu\omega_0\delta t\ll 1$, which confirms numerical result and shows that $d_{(x),\max}^{\delta t}$ can also be made much smaller than $d_x=1/S$, similar to the result for $d_{(x)}$.

Overall, the analytical and numerical results show that the feedback is sufficiently efficient for a broad range of feedback parameters F and μ .

At the end of this section we would like to discuss the following concern on the possibility of using the quantum feedback in the case of stroboscopic measurements. The general idea of stroboscopic QND measurement is to avoid obtaining any information on phase of the nanoresonator oscillations, while quantum feedback requires us to know the phase of packet center oscillations. So, a natural question is how it happens that we monitor this phase.

A qualitative answer is that once we know $\langle x \rangle$ and $\langle p \rangle$, their further evolution can be extracted from the measurement record $I(t)$ via Eqs. (26) and (27) even though the measurement is performed during only a small fraction of the period. (During “off” phases the evolution is deterministic and feedback is still continuously applied based on oscillating calculated values of $\langle x \rangle$ and $\langle p \rangle$.) Initial knowledge of $\langle x \rangle$ and $\langle p \rangle$ can be eventually obtained also using Eqs. (26) and (27) starting from any (incorrect) initial condition, since the solution of the equations gradually forgets initial condition and is eventually dominated by the noise term known from the measurement record.

Let us assume that we start using Eqs. (26) and (27) with “incorrect” initial conditions $\langle x_1(0) \rangle$ and $\langle p_1(0) \rangle$ instead of “correct” values $\langle x_2(0) \rangle$ and $\langle p_2(0) \rangle$, and let us show that the

normalized differences between the corresponding solutions $\tilde{x} = (\langle x_1 \rangle - \langle x_2 \rangle) / \sqrt{\hbar/2m\omega_0}$ and $\tilde{p} = (\langle p_1 \rangle - \langle p_2 \rangle) / \sqrt{\hbar m\omega_0/2}$ decay to zero with time. Since the same measurement record $I(t)$ is used for both solutions, the value of the noise term $\xi = I - \langle I \rangle$ is affected by \tilde{x} , and the difference evolves as

$$d\tilde{x}/dt = \omega_0[\tilde{p} - C_0 f(t)] d_x \tilde{x}, \quad (75)$$

$$d\tilde{p}/dt = \omega_0[-\tilde{x} - C_0 f(t)] d_{xp} \tilde{x} - \tilde{p}/Q. \quad (76)$$

Finite Q -factor obviously damps oscillations of \tilde{x} and \tilde{p} , so for a worst case let us assume $Q = \infty$. Then the evolution of the “energy function” $\tilde{\varepsilon} = \tilde{x}^2 + \tilde{p}^2$ is $d\tilde{\varepsilon}/dt = -2\omega_0 C_0 f(t) [(d_x \tilde{x}^2 + d_{xp} \tilde{x} \tilde{p})]$. Assuming weak coupling, using asymptotic time dependence of variances $d_x = S^{-1} + A[1 - \cos(2\omega_0 t)]$, $d_{xp} = A \sin(2\omega_0 t)$ [see Eqs. (36) and (38)], and assuming $\tilde{x} = \tilde{\varepsilon}^{1/2} \sin(\omega_0 t + \phi)$, $\tilde{p} = \tilde{\varepsilon}^{1/2} \cos(\omega_0 t + \phi)$, we derive equation $d\tilde{\varepsilon}/dt = -\tilde{\varepsilon} \omega_0 C_0 f(t) \{ (A + S^{-1}) [1 - \cos(2\omega_0 t + 2\phi)] - A [\cos(2\omega_0 t) - \cos(2\phi)] \}$. After averaging over the short pulse duration δt , the expression in curly brackets becomes $A [1 + \cos(2\phi)] (\omega_0 \delta t)^2 / 6 + S^{-1} [1 - \cos(2\phi)] (1 - (\omega_0 \delta t)^2 / 6)$, which is always positive. Therefore, $\tilde{\varepsilon}$ decays to zero, and this happens on the time scale $\sim T_0 \eta^{1/2} C_0^{-1} (\omega_0 \delta t)^{-2}$, comparable to the timescale of purity saturation and squeezing buildup (see Sec. IV C). So, we have proven that $\langle x \rangle$ and $\langle p \rangle$ calculated from Eqs. (26) and (27) eventually depend only on the measurement record and do not depend on initial values. As a by-product, this statement also means that a mixture of Gaussian states (which in general is not Gaussian) eventually becomes a single Gaussian state.

VI. VERIFICATION OF SQUEEZED STATE

The fact that the squeezed state of a nanoresonator can be prepared by the modulated measurement and quantum feedback, does not automatically mean that this state may be useful for the measurement of extremely weak forces, and even that such state can be checked experimentally in a straightforward way. As an example of such problem, in one of setups analyzed in Ref. 63 the squeezed in-loop optical state is realized by using quantum feedback, but the squeezing of the output light is impossible. Fortunately, as we discuss below, in our case there is no problem with observability of the squeezed state.

We have studied the possibility to verify the squeezed state of the nanoresonator in the following way. After the preparation of the squeezed state by stroboscopic measurement and feedback, the feedback at some moment ($t=0$) is switched off, while the stroboscopic measurement continues. Considering for simplicity the case of one measurement per nanoresonator period ($n=2, \omega = \omega_0$), we average the position measurement result x_j^m for the j th pulse over many pulses (each pulse gives a very imprecise result because of weak coupling):

$$X_N = \frac{1}{N} \sum_{j=1}^N x_j^m = \frac{1}{N} \sum_{j=1}^N \frac{1}{\delta t k_0} \int_{jT_0 - \delta t/2}^{jT_0 + \delta t/2} [I(t) - I_{00}] dt. \quad (77)$$

As we show below, for a squeezed initial state, the r.m.s. fluctuation of X_N can be much smaller than if we would start

with the ground state (and much smaller than Δx_0). This is the way to verify squeezing, and also this procedure is exactly what can be used for an ultrasensitive force measurement with accuracy beyond the standard quantum limit. [Notice that for two measurements per period, $\omega = 2\omega_0$, the definition (77) should be modified by adding odd (“ π -phase”) contributions with negative sign. Then all results of this section are valid for $\omega = 2\omega_0$ as well.] For simplicity in this section we neglect the effect of finite quality factor Q of the nanoresonator.

The analysis of the distribution of X_N (over realizations) is very simple in the case of instantaneous but imprecise measurements, $\delta t \rightarrow 0$, $C_0 \delta t = \text{const}$, since the Hamiltonian evolution of the resonator in between the measurements can be completely neglected. Therefore the problem reduces to a classical sequential measurement of a “particle” position, which is initially characterized by the Gaussian probability distribution with variance $\Delta x_0^2/S$ (recall $\Delta x_0 = \sqrt{\hbar/2m\omega_0}$), while each imprecise measurement has variance $(\Delta x_0)^2/C_0 \omega_0 \delta t$. In particular, N measurements with results x_j^m are equivalent to one N -times stronger measurement with result X_N [mathematically this is because the product of several measurement Gaussians as in Eq. (9) is the Gaussian with added inverse variances and centered at X_N]. Then distribution of X_N is the convolution of the initial state Gaussian and the total measurement Gaussian [see Eq. (7)]; so the variance $D_{X,N}$ of X_N is equal to the sum of corresponding variances,

$$D_{X,N} = \Delta x_0^2 \left(\frac{1}{S} + \frac{1}{NC_0 \omega_0 \delta t} \right). \quad (78)$$

For completeness let us also mention that after N measurements the “actual” position is characterized by the Gaussian probability [see Eq. (9)] with variance $\Delta x_0^2 (S + NC_0 \omega_0 \delta t)^{-1}$ (inverse variances are added for product of Gaussians) and centered at $X_N / (1 + S/NC_0 \omega_0 \delta t)$, which is the weighted sum of the initial center of distribution (assumed to be zero) and the measurement result X_N .

Obviously, at $N \gg 1/C_0 \omega_0 \delta t$ the variance of X_N given by Eq. (78) is significantly smaller for a squeezed state ($S > 1$) than for the ground state ($S = 1$). Even though this difference can be rigorously verified only by performing many experiments to accumulate statistics for $D_{X,N}$, it can be observed even in a single experiment with good reliability if $S \gg 1$ (for applications like force detection we should discuss single realizations). The error probability for distinguishing between the two cases in one trial is essentially the overlap of two distributions for X_N , which is crudely $S^{-1/2}$ for $N \rightarrow \infty$ (ratio of distribution widths). [A better approximation for error probability to distinguish between two Gaussians with coinciding centers and different variances D_1 and D_2 is $(\ln R/2\pi R)^{1/2}$ where $R = D_1/D_2 \gg 1$; in our case $R = S$.] So, the squeezed state with $S \gg 1$ can be reliably verified even in a single experiment.

Unfortunately, this result requires the assumption of infinitely strong coupling with detector ($C_0 \rightarrow \infty$), so it is not obvious if it holds in the practical case of weak coupling ($C_0 \ll 1$) or not. The anticipated problem is that for suffi-

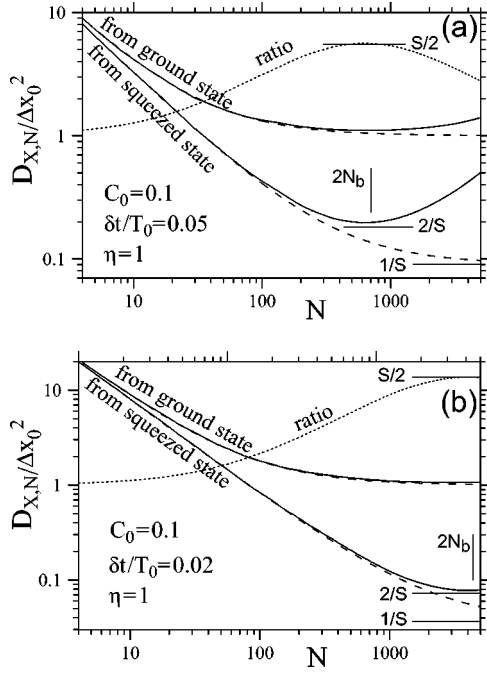


FIG. 10. Variance $D_{X,N}$ of the measurement result X_N [see Eq. (77)] as a function of number N of stroboscopic measurement pulses. The measurement procedure is applied either to the ground state or to the squeezed state prepared by the same procedure complemented with quantum feedback. Panels (a) and (b) are for different durations of the measurement pulses, corresponding to initial squeezing $S=11.0$ and $S=27.6$. Solid lines are the numerical results for finite pulse duration δt , while dashed lines correspond to Eq. (78) (instantaneous measurements). Dotted lines are the ratios of the results shown by solid lines. Force detection beyond the standard quantum limit is possible when $D_{X,N}/\Delta x_0^2 < 1$.

ciently large N which makes the second term in Eq. (78) sufficiently small, the nanoresonator heating due to measurement backaction may already eliminate the squeezing (the feedback is off). To resolve this issue we have calculated $D_{X,N}$ for stroboscopic modulation numerically by Monte Carlo simulation of realizations using Eqs. (26) and (27) and then averaging over realizations. Such simulation happened to be not too simple; in particular, the time step should be chosen carefully. As a check of the simulation accuracy we were comparing the variance of $\langle x \rangle$ obtained by averaging over Monte Carlo realizations with the results from Eqs. (69)–(71) without feedback; the difference was checked to be within a few percent.

Solid lines in Fig. 10 show the numerical results for $D_{X,N}$ for weak coupling ($C_0=0.1$) and two values of pulse duration: (a) $\delta t/T_0=0.05$ and (b) $\delta t/T_0=0.02$. The initial state is either ground state or asymptotic zero-centered squeezed state corresponding to the same measurement parameters, so that the squeezing is given by Eq. (52) and preparation of the squeezed state differs from its verification only by quantum feedback switched on or off. Dashed lines in Fig. 10 are calculated using Eq. (78). One can see that the numerical results follow the simple analytics when the contribution from the measurement accuracy in Eq. (78) dominates; however, at larger number of pulses N the numerical results de-

viate upwards and eventually $D_{X,N}$ starts to increase with N , which is expected because of the nanoresonator “heating” due to measurement back-action.

The numerical minimum of $D_{X,N}$ for squeezed states ($S \gg 1$) in Fig. 10 is a little higher than $(2/S)\Delta x_0^2$. We have checked that the minimum is still close to $(2/S)\Delta x_0^2$ for several other values of C_0 and δt . As seen in Fig. 10, this minimum is achieved at N close to $2N_b$, where N_b given by Eq. (55) is the estimate of number of measurement pulses for squeezing buildup. We have checked that this result also holds for different values of C_0 and δt . The fact that the minimum of $D_{X,N}$ is higher than $(2/S)\Delta x_0^2$ is not surprising since the average variance D_x (square of the wave packet width) within the pulse duration δt is $(2/S)\Delta x_0^2$ for $S \gg 1$ (see Sec. IV B 3). Hence, one could even guess that $D_{X,N}$ should be always larger than Eq. (78) with $1/S$ replaced by $2/S$. However, actually $D_{X,N}$ goes below such a bound for a range of N . Some understanding of this fact can be provided by an argument that for a classical measurement the nanoresonator motion during δt would be averaged and so X_N would depend only on the nanoresonator position at the centers of the measurement pulses.

The minimum of $D_{X,N}$ for the case when we start measurement procedure from the ground state, is only a little larger than Δx_0^2 (see Fig. 10), which means that the accumulated measurement accuracy becomes better than the standard quantum limit Δx_0 at sufficiently smaller N than when the back-action heating becomes important. Therefore, the ratio of $D_{X,N}$ starting with the ground and squeezed states (dotted lines in Fig. 10) reaches the maximum of approximately $S/2$ [in the case of instantaneous measurements described by Eq. (78), this ratio would approach S at $N \rightarrow \infty$].

Thus, our numerical results show that for a proper duration of the measurement procedure ($\sim N_b T_0$) the variances $D_{X,N}$ for the squeezed and ground initial states are significantly different, and therefore these states can be reliably distinguished. The squeezed state verification using a weakly coupled detector is only by a factor ~ 2 less efficient than a similar procedure using instantaneous measurements by a strongly coupled detector. Even though these results have been obtained neglecting the effect of the resonator Q -factor, we do not expect a significant difference for finite Q because it equally affects the preparation of the squeezed state and its verification. Finally, let us mention that if an external force has shifted the nanoresonator position by Δx , the procedure discussed in this section can detect the force if $\Delta x \gtrsim \sqrt{2/S}\Delta x_0$.

VII. CONCLUSION

As analyzed in this paper, the uncertainty of the nanoresonator position can be squeezed significantly below the ground state level by using the modulated in time ($\omega \approx 2\omega_0/n$) continuous measurement of the nanoresonator position with the QPC or RF-SET detector. The measurement strength can be modulated by applying the periodic voltage across the detector. For the RF-SET the modulation can also be done by varying the gate voltage; however, it is important that such modulation periodically brings the SET into the

Coulomb blockade regime, so that the back-action is periodically switched off (actually, similar gate voltage modulation is also possible for the QPC, but it is quite unnatural). The mechanism of squeezing is similar to the stroboscopic QND measurements:^{8,12,13} for periodic measurement pulses separated by integer number of half-periods of oscillation, the free evolution of the resonator is to the large extent compensated, which allows the buildup of the effective measurement strength for repeated imprecise measurements; therefore the squeezed state is produced when effective measurement accuracy becomes better than the ground state width Δx_0 . A significant difference between our analysis and the standard QND case of instantaneous stroboscopic measurements is the assumption of weak coupling with detector, $C_0 \lesssim 1$, while C_0 should be infinitely large for instantaneous measurements. Obviously, the squeezed state oscillates with time, so that the moments of minimum position uncertainty $\Delta x_0/\sqrt{S}$ and the minimum momentum uncertainty $\hbar/2\Delta x_0\sqrt{S}$ are shifted in time by $T_0/4 = \pi/2\omega_0$.

We have considered harmonic (22) and stroboscopic (23) modulations with frequency ω and modulation amplitude A_{mod} . As anticipated, $A_{\text{mod}}=1$ is found to be the optimum value for maximum squeezing in both cases. We have found that only a moderate squeezing $S = \sqrt{3}\eta$ (requiring relatively high detector quantum efficiency η) is possible for the harmonic modulation with twice the resonator frequency, $\omega = 2\omega_0$ [see Eqs. (40), (41), and (43), and Fig. 3]. In contrast, an arbitrary strong squeezing is in principle possible for the stroboscopic modulation when the measurement (and therefore back-action) is switched completely off in between measurement pulses of short duration δt . If not limited by effects of resonator quality factor Q , the squeezing can be up to $S = 2\sqrt{3}\eta/\omega_0\delta t$ at frequency $\omega = 2\omega_0/n$ [see Eqs. (50)–(53) and Figs. 4 and 5]. The squeezing buildup requires on the order of $\sqrt{\eta/C_0}(\omega_0\delta t)^2$ measurement pulses [see Eq. (55)], so for a limited “waiting time” τ_w the squeezing cannot exceed $S \approx 2\eta^{1/4}(C_0\tau_w/T_0)^{1/2}$ [see Fig. 7 and Eqs. (58)–(60)]. Finite Q -factor of the nanoresonator limits the squeezing by $S = [(2/n)(\omega_0\delta t/2\pi)C_0Q/\coth(\hbar\omega_0/2T)]^{1/2}$ [see Eq. (66)]; after optimization over δt this leads to the limitation $S \approx (3/4)[\sqrt{\eta}C_0Q/n\coth(\hbar\omega_0/2T)]^{1/3}$ [see Fig. 8 and Eq. (65)]. Notice that this result is consistent with the mentioned in the Introduction condition of quantum behavior⁸ $T\tau_m/Q \lesssim \hbar$ for a good detector, $\eta \sim 1$, and measurement time $\tau_m = 4/C_0\omega_0$ corresponding to x -accuracy equal to Δx_0 .

While the modulated measurement squeezes the width of the resonator wave packet, the position of its center $\langle x \rangle$ fluctuates due to random back-action from the detector, and may deviate very far away from the origin. To keep the packet center near $x=0$ we apply quantum feedback similar to Refs. 33 and 30 (the packet center in momentum space in this case will be kept near zero as well). We have found [see Fig. 9 and Eqs. (73) and (74)] that the feedback can keep the deviation of $\langle x \rangle$ from zero at the level much smaller than the packet width $\Delta x_0/\sqrt{S}$, which means that the ensemble-averaged squeezing practically does not differ from the packet width squeezing.

Verification of the squeezed state can be performed in essentially the same way as its preparation, the only differ-

ence is that the quantum feedback should be switched off. We have studied the distribution of the position measurement result X_N averaged over N stroboscopic measurement pulses and found (see Fig. 10) that for a significant range of N before the back-action heating becomes important, the width of X_N distribution is close to $\sqrt{2/S}\Delta x_0$, which may be much smaller than the ground state width Δx_0 . The analyzed procedure can be applied in a straightforward way for ultrasensitive force detection beyond the standard quantum limit: the force can be detected when it causes the nanoresonator shift Δx larger than $\sqrt{2/S}\Delta x_0$.

For an estimate of the present-day experimental parameters let us use the data from Ref. 5. The experimental sensitivity of 3.8 fm/ $\sqrt{\text{Hz}}$ for the nanoresonator with $\omega_0/2\pi = 19.7$ MHz and $\Delta x_0 = 21$ fm can be translated into the dimensionless coupling $C_0 \approx 5 \times 10^{-7}$. For the Q -factor of 3.5×10^4 and using a crude estimate for quantum efficiency $\eta \sim 10^{-1}$, we have the product $C_0Q\sqrt{\eta} \approx 6 \times 10^{-2}$. Since this product should be larger than at least 10 for a noticeable squeezing (see Fig. 8), we should conclude that it is still 2–3 orders of magnitude less than needed for squeezing. However, the necessary improvement of experimental parameters may be reachable in a reasonably near future (notice that C_0 scales quadratically with response k_0 ; the estimates of Ref. 30 give $C_0 \approx 10^{-3}$). (Recently one of the authors succeeded in fabrication of a 30 MHz resonator with low-temperature Q -factor of 2.3×10^5 and a 9.8 MHz resonator with $Q = 1.5 \times 10^5$). For reasonably realistic parameters $C_0 \sim 10^{-2}$, $Q \sim 10^6$, and $\eta \sim 0.3$ the product $C_0Q\sqrt{\eta} \approx 5 \times 10^3$, therefore the low-temperature squeezing $S \approx 13$ is possible, and a significant squeezing survives up to temperatures $T \sim 10\hbar\omega_0$.

In an experiment it may be convenient to flip every second time the sign of stroboscopic voltage pulse applied to the detector. Then the information about the average position X_N [see Eq. (77)] can be extracted from the low-frequency component of the detector current (somewhat similar to the RF-SET mixer of Ref. 4). Even though we expect that the high-frequency component would still be necessary for quantum feedback, the results of Sec. VI indicate that the preparation-detection procedure should work reasonably well even without feedback if the preparation time is comparable to the squeezing buildup time (so that the back-action heating is not yet too strong).

Concluding, we hope that the QND squeezing of a nanoresonator can be demonstrated experimentally in a reasonably near future and will eventually be useful for the force detection with sensitivity beyond the standard quantum limit.

ACKNOWLEDGMENTS

The authors would like to thank D. Averin, A. Doherty, S. Habib, K. Jacobs, K. Likharev, I. Martin, A. Matsko, and G. Milburn for fruitful discussions and remarks. The work was supported by NSA and ARDA under ARO Grants Nos. DAAD19-01-1-0491 and W911NF-04-1-0204 (R.R. and A.N.K.) and by NSA (K.S.).

APPENDIX: GENERALIZED BAYESIAN FORMALISM FOR A NANORESONATOR

In this Appendix we generalize the Bayesian equation (18) to the case of a detector with correlation between output

and back-action noises, and also discuss the contributions from various kinds of the noise. We discuss only the nanoresonator evolution due to measurement; therefore the terms \mathcal{H}_0 , \mathcal{H}_{env} , and \mathcal{H}_{fb} in the Hamiltonian (1) are neglected. For simplicity we also do not consider the modulation of measurement parameters.

Following the logic of Ref. 45, we discuss first the effects of several additional classical noises. Let us start with additional classical white noise $\xi_1(t)$ at the output, so that the total output noise $\xi = \xi_{\text{id}} + \xi_1$ consists of the “ideal quantum contribution” ξ_{id} discussed in Sec. II [see Eq. (17)] and ξ_1 ; the corresponding spectral densities are $S_I = S_{\text{id}} + S_1$. Using the “double Bayesian” procedure of Ref. 45 it is simple to show that averaging over ξ_1 leads to the addition of the decoherence term $-\gamma_1(x-x')^2\rho(x,x')$ with $\gamma_1 = k^2 S_1 / 4S_{\text{id}} S_I$ into Eq. (17). Therefore, the effect of ξ_1 is the reduction of the quantum efficiency η from the ideal value $\eta = 1$ down to $\eta = S_{\text{id}} / S_I$.

The second natural noise source is the classical force $\xi_2(t)$ (uncorrelated with ξ_1) with white spectral density S_2 , which leads to the stochastic term $-\xi_2(t)\hat{x}$ in the Hamiltonian. Averaging over ξ_2 gives the extra decoherence term $-\gamma_2(x-x')^2\rho(x,x')$ in Eq. (17) with $\gamma_2 = S_2 / 4\hbar^2$. Therefore the effect of ξ_2 can still be taken into account by further reduction of the efficiency η .

When the nanoresonator is measured by a single-electron transistor, the back-action force is in general correlated with the output noise. To take this correlation into account, let us introduce one more stochastic classical force $\xi_3(t) = \alpha\xi_1(t)$ fully correlated with output noise ξ_1 (this obviously accounts for arbitrary correlation between the total force $\xi_2 + \xi_3$ and ξ_1). Averaging over ξ_3 leads to the terms

$$i\mathcal{K}(x-x')\rho(x,x')\xi(t) - (\gamma_3 + \mathcal{K}^2 S_I / 4)(x-x')^2\rho(x,x') \quad (\text{A1})$$

with correlation factor $\mathcal{K} = \alpha S_1 / \hbar S_I$ and decoherence $\gamma_3 = \alpha^2 S_{\text{id}} S_1 / 4\hbar^2 S_I$ to be added into Eq. (17). [Notice that Eq. (17) is in the Itô form; there is no contribution $\mathcal{K}^2 S_I / 4$ to decoherence in the Stratonovich form.] The correlation term cannot be described in terms of efficiency η and requires generalization of the Bayesian equation (18).

For measurement by single-electron transistor the average back-action force actually depends on the nanoresonator position x in a rather complicated way, and this leads to additional potential energy term $\mathcal{V}_{\text{add}}(\hat{x})$ in the Hamiltonian. In general this term contributes to unharmonicity of the nanoresonator, though for small amplitude of oscillations it mainly shifts the equilibrium point and renormalizes the spring constant.

The effects of correlation between the output and back-action noises are also important for a detector with “asymmetric” coupling described by nonzero relative phase^{43–45} between complex magnitudes M and ΔM in the Hamiltonian terms (4) and (5). Evolution equation (17) for such a detector should be complemented^{44,45} by the terms similar to Eq. (A1) with correlation factor $\mathcal{K} = e^{-1} |\Delta M / M| \sin[\arg(\Delta M / M)]$ but without dephasing, $\gamma_3 = 0$ (the detector is still ideal in the sense that a pure state of the nanoresonator remains pure in the course of measurement). Besides the correlation term, the oscillator potential is changed by the contribution $\mathcal{V}_{\text{add}}(x) = -\hbar\mathcal{K}(I_0 + kx)^2 / 2k + \text{const.}$

For completeness let us also consider the noise of the spring constant described by the stochastic potential energy $\xi_4 x^2$. Averaging over this noise leads to the term $-\gamma_{\text{spr}}(x^2 - x'^2)^2\rho(x,x')$ (where $\gamma_{\text{spr}} = S_4 / 4\hbar^2$) which has significantly different form compared to the standard decoherence term (in particular, this term makes the density matrix non-Gaussian).

Combining all contributions, the nanoresonator evolution due to measurement is described in Itô form as

$$\begin{aligned} \dot{\rho}(x,x') = & - \left(\frac{k^2}{4S_I} + \frac{\mathcal{K}^2 S_I}{4} + \gamma_d \right) (x-x')^2 \rho(x,x') \\ & + \left(\frac{k}{S_I} (x+x' - 2\langle x \rangle) + i\mathcal{K}(x-x') \right) \rho(x,x') \xi(t) \\ & + [\mathcal{V}_{\text{add}}(\hat{x}), \rho]_{x,x'} - \gamma_{\text{spr}} (x^2 - x'^2)^2 \rho(x,x'), \quad (\text{A2}) \end{aligned}$$

where \mathcal{K} is the total correlation factor, γ_d is the total dephasing, γ_{spr} is due to noise of the spring constant, and $\mathcal{V}_{\text{add}}(x)$ is the renormalization of the resonator potential energy.

*On leave of absence from Institute for Nuclear Research and Nuclear Energy, Sofia BG-1784, Bulgaria; Present address: Physics Department, Pennsylvania State University, University Park, Pennsylvania 16802.

¹A. N. Cleland and M. L. Roukes, *Appl. Phys. Lett.* **69**, 2653 (1996); A. N. Cleland and M. L. Roukes, *Nature (London)* **392**, 160 (1998); E. Buks and M. L. Roukes, *Europhys. Lett.* **54**, 220 (2001).

²D. W. Carr and H. G. Craighead, *J. Vac. Sci. Technol. B* **15**, 2760 (1997); H. G. Craighead, *Science* **290**, 1532 (2000); M. Zalalutdinov, B. Ilic, D. Czaplewski, A. Zehnder, H. G. Craighead, and J. M. Parpia, *Appl. Phys. Lett.* **77**, 3287 (2000).

³X. Ming, H. Huang, C. A. Zorman, M. Mehregany, and M. L. Roukes, *Nature (London)* **421**, 496 (2003).

⁴R. G. Knobel and A. N. Cleland, *Nature (London)* **424**, 291 (2003).

⁵M. D. LaHaye, O. Buu, B. Camarota, and K. C. Schwab, *Science* **304**, 74 (2004).

⁶A. Cleland, *Foundations of Nanomechanics* (Springer, Berlin, 2003).

⁷M. Blencowe, *Phys. Rep.* **395**, 159 (2004).

⁸V. B. Braginsky and F. Ya. Khalili, *Quantum Measurement* (Cambridge University Press, Cambridge, 1992).

⁹A. N. Cleland, J. S. Aldridge, D. C. Driscoll, and A. C. Gossard,

- Appl. Phys. Lett. **81**, 1699 (2002).
- ¹⁰D. Rugar, R. Budakian, H. J. Mamin, and B. W. Chul, Nature (London) **430**, 329 (2004); J. A. Sidles, J. L. Garbini, K. J. Bruland, D. Rugar, O. Züger, S. Hoen, and C. S. Yannoni, Rev. Mod. Phys. **67**, 249 (1995).
- ¹¹I. Tittonen, G. Breitenbach, T. Kalkbrenner, T. Müller, R. Conradt, S. Schiller, E. Steinsland, N. Blanc, and N. F. de Rooij, Phys. Rev. A **59**, 1038 (1999).
- ¹²V. B. Braginsky, Yu. I. Vorontsov and F. Ya. Khalili, JETP Lett. **27**, 276 (1978).
- ¹³K. S. Thorne, R. W. P. Drever, C. M. Caves, M. Zimmermann, and V. D. Sandberg, Phys. Rev. Lett. **40**, 667 (1978).
- ¹⁴C. M. Caves, K. S. Thorne, R. W. P. Drever, V. D. Sandberg, and M. Zimmermann, Rev. Mod. Phys. **52**, 341 (1980).
- ¹⁵M. F. Bocko and R. Onofrio, Rev. Mod. Phys. **68**, 755 (1996).
- ¹⁶H. J. Kimble, Y. Levin, A. B. Matsko, K. S. Thorne, and S. P. Vyatchanin, Phys. Rev. D **65**, 022002 (2002).
- ¹⁷V. B. Braginskii, Phys. Usp. **46**, 81 (2003).
- ¹⁸A. B. Matsko and S. P. Vyatchanin, Appl. Phys. B: Lasers Opt. **64**, 167 (1997).
- ¹⁹D. V. Averin, Phys. Rev. Lett. **88**, 207901 (2002).
- ²⁰L. Bulaevskii, M. Hruska, A. Shnirman, D. Smith, and Y. Makhlin, Phys. Rev. Lett. **92**, 177001 (2004).
- ²¹A. N. Jordan and M. Büttiker, Phys. Rev. B **71**, 125333 (2005)..
- ²²J. M. Geremia, J. K. Stockton, and H. Mabuchi, Science **304**, 270 (2004).
- ²³R. Ruskov, K. Schwab, and A. N. Korotkov, IEEE Transactions on Nanotechnology **4**, 132 (2005).
- ²⁴M. P. Blencowe, and M. N. Wybourne, Appl. Phys. Lett. **77**, 3845 (2000); A. D. Armour, M. P. Blencowe, and Y. Zhang, Phys. Rev. B **69**, 125313 (2004).
- ²⁵D. Mozyrsky and I. Martin, Phys. Rev. Lett. **89**, 018301 (2002).
- ²⁶A. D. Armour, M. P. Blencowe, and K. C. Schwab, Phys. Rev. Lett. **88**, 148301 (2002).
- ²⁷A. Y. Smirnov, L. G. Mourokh, and N. J. M. Horing, Phys. Rev. B **67**, 115312 (2003).
- ²⁸K. Schwab, Appl. Phys. Lett. **80**, 1276 (2002).
- ²⁹R. Knobel and A. N. Cleland, Appl. Phys. Lett. **81**, 2258 (2002).
- ³⁰A. Hopkins, K. Jacobs, S. Habib, and K. Schwab, Phys. Rev. B **68**, 235328 (2003).
- ³¹Ya. M. Blanter, O. Usmani, and Yu. V. Nazarov, Phys. Rev. Lett. **93**, 136802 (2004).
- ³²A. A. Clerk, Phys. Rev. B **70**, 245306 (2004).
- ³³A. C. Doherty and K. Jacobs, Phys. Rev. A **60**, 2700 (1999).
- ³⁴I. Martin, A. Shnirman, L. Tian, and P. Zoller, Phys. Rev. B **69**, 125339 (2004).
- ³⁵I. Wilson-Rae, P. Zoller, and A. Imamoglu, Phys. Rev. Lett. **92**, 075507 (2004).
- ³⁶R. Ruskov and A. N. Korotkov, Phys. Rev. B **66**, 041401(R) (2002); A. N. Korotkov, cond-mat/0404696 (unpublished).
- ³⁷H. M. Wiseman and G. J. Milburn, Phys. Rev. Lett. **70**, 548 (1993).
- ³⁸M. P. Blencowe and M. N. Wybourne, Physica B **280**, 555 (2000).
- ³⁹L. P. Grishchuk and M. V. Sazhin, Sov. Phys. JETP **57**, 1128 (1983).
- ⁴⁰D. Rugar and P. Grütter, Phys. Rev. Lett. **67**, 699 (1991).
- ⁴¹P. Rabl, A. Shnirman, and P. Zoller, Phys. Rev. B **70**, 205304 (2004).
- ⁴²S. A. Gurvitz, Phys. Rev. B **56**, 15215 (1997).
- ⁴³A. N. Korotkov and D. V. Averin, Phys. Rev. B **64**, 165310 (2001).
- ⁴⁴H. S. Goan and G. J. Milburn, Phys. Rev. B **64**, 235307 (2001).
- ⁴⁵A. N. Korotkov, Phys. Rev. B **67**, 235408 (2003).
- ⁴⁶W. Mao, D. V. Averin, R. Ruskov, and A. N. Korotkov, Phys. Rev. Lett. **93**, 056803 (2004).
- ⁴⁷A. N. Korotkov, Phys. Rev. B **60**, 5737 (1999); **63**, 115403 (2001).
- ⁴⁸T. Bayes, Philos. Trans. R. Soc. London **53**, 370 (1763); P. S. Laplace, *Théorie analytique des Probabilités* (Ve Courcier, Paris, 1812); E. Borel, *Elements of the Theory of Probability* (Prentice-Hall, Englewood Cliffs, 1965).
- ⁴⁹A. O. Caldeira and A. J. Leggett, Ann. Phys. (N.Y.) **149**, 374 (1983); Physica A **121**, 587 (1983).
- ⁵⁰J. von Neumann, *Mathematical Foundations of Quantum Mechanics* (Princeton University Press, Princeton, 1955).
- ⁵¹B. Øksendal, *Stochastic Differential Equations* (Springer, Berlin, 1998).
- ⁵²M. B. Mensky, Phys. Usp. **168**, 1017 (1998).
- ⁵³M. J. Gagen, H. M. Wiseman, and G. J. Milburn, Phys. Rev. A **48**, 132 (1993).
- ⁵⁴G. Lindblad, Commun. Math. Phys. **48**, 119 (1976).
- ⁵⁵C. M. Caves and G. J. Milburn, Phys. Rev. A **36**, 5543 (1987).
- ⁵⁶W. H. Zurek, S. Habib, and J. P. Paz, Phys. Rev. Lett. **70**, 1187 (1993).
- ⁵⁷D. V. Averin, Fortschr. Phys. **48**, 1055 (2000).
- ⁵⁸C. W. Gardiner, *Quantum Noise* (Springer-Verlag, Berlin, 1991).
- ⁵⁹A. O. Caldeira, H. A. Cerdeira, and R. Ramaswamy, Phys. Rev. A **40**, 3438 (1989).
- ⁶⁰J. Halliwell and A. Zoupas, Phys. Rev. D **52**, 7294 (1995).
- ⁶¹J. K. Breslin and G. J. Milburn, Phys. Rev. A **55**, 1430 (1997).
- ⁶²V. V. Dodonov, E. V. Kurmyshev, and V. I. Man'ko, Phys. Lett. **79**, 150 (1980).
- ⁶³H. M. Wiseman and G. J. Milburn, Phys. Rev. A **49**, 1350 (1994).